

Report 10, 1991

**PRODUCTION CHARACTERISTICS OF THE  
MOMOTOMBO GEOTHERMAL FIELD, NICARAGUA**

Enrique Porras Mendieta,  
UNU Geothermal Training Programme,  
Orkustofnun - National Energy Authority,  
Grensasvegur 9,  
108 Reykjavik,  
ICELAND

Permanent address:  
Recursos Geotérmicos (INE),  
Casa Nazareth 1c. al Lago,  
Apartado Postal No. 2817,  
Managua,  
NICARAGUA

**ABSTRACT**

An analysis and interpretation is given of eight years of fluid production from the Momotombo high temperature field, Nicaragua. The study consisted of a careful analysis of the measurement methods used to estimate total flowrates and enthalpies from geothermal wells. Then, all available production data from Momotombo were collected and plotted with time. The cumulative production from the field was also calculated. Based on these calculations, a volumetric analysis was performed.

The eight years of production have induced a pressure drawdown of more than 20 bars in the shallower part of the Momotombo reservoir. The drawdown has initiated extensive boiling in the reservoir. Now three zones of reservoir conditions can be found in the initially liquid-saturated reservoir; a dry steam zone between approximately 150 - 250 m b.s.l., a two-phase zone between 250 and 320 m b.s.l., and a saturated liquid zone at depths greater than 320 m b.s.l..

The cumulative mass production from the field is on the order of 60 million tons. Volumetric analysis of fluid in storage indicates that 40% of the produced mass has been taken from the shallow reservoir, 35% is fed by natural recharge to the system and 25% by reinjection and production from deep reservoir wells. If these proportions remain the same in the future, only 6 to 10 years may pass until the shallow reservoir is fully depleted.

## TABLE OF CONTENTS

	Page
ABSTRACT .....	3
TABLE OF CONTENTS .....	4
LIST OF FIGURES .....	5
LIST OF TABLES .....	5
1. INTRODUCTION .....	6
1.1 Statement of the problem .....	6
1.2 Outline of the Momotombo geothermal field .....	6
1.3 Data sources .....	7
2. DISCHARGE MEASUREMENTS OF TWO-PHASE WELLS .....	9
2.1 The lip pressure method .....	9
2.2 The steam separator method .....	11
2.2.1 Steam flowrate measurement .....	11
2.2.2 Water flowrate measurement .....	15
2.2.3 Total enthalpy and flowrate from the well .....	17
3. PRODUCTION MONITORING IN THE MOMOTOMBO GEOTHERMAL FIELD .....	18
3.1 Outline of the production history .....	18
3.2 Production data from the individual wells .....	20
3.3 Reinjection data .....	27
4. ANALYSIS ON THE PRODUCTION DATA .....	28
4.1 Daily and cumulative production .....	28
4.2 Pressure drawdown and permeability .....	31
4.3 Enthalpy changes in initially liquid-saturated reservoirs .....	33
4.3.1 Extensive boiling .....	34
4.3.2 Mobility effects .....	34
4.4 Interpretation of enthalpy changes in the Momotombo reservoir .....	37
5. VOLUMETRIC MASS CALCULATIONS .....	39
5.1 Initial mass in storage .....	39
5.2 Natural recharge .....	40
5.3 Future performance of the shallow reservoir .....	41
6. CONCLUSIONS AND RECOMMENDATIONS .....	43
ACKNOWLEDGEMENTS .....	44
NOMENCLATURE .....	45
REFERENCES .....	47
APPENDIX I: List of programs (LIP, CUM, MOM and KASAP) .....	49

## LIST OF FIGURES

	Page
1. Location of the Momotombo geothermal field within the Coordillera Los Marrabios volcanic complex in Nicaragua .....	7
2. Annual electricity production from the two electrical units .....	8
3. Typical wellhead equipment used to measure flowrate and enthalpy by the Russel James method .....	10
4. A sketch of a cyclone separator .....	11
5. A sketch of a thin-plate orifice in a flowline and the location of pressure taps .....	12
6. The discharge coefficient $C_d$ for corner taps .....	14
7. Reynolds number for different steam flowrates .....	15
8. A sketch of a weir box .....	16
9. Areal map of the Momotombo geothermal field .....	18
10. Production history of well MT-2 .....	20
11. Output curve for well MT-9 in November 1988 .....	21
12. Production history of well MT-12 .....	21
13. Production history of well MT-17 .....	22
14. Production history of well MT-20 .....	23
15. Production history of well MT-22 .....	23
16. Production history of well MT-23 .....	24
17. Production history of well MT-26 .....	24
18. Production history of well MT-27 .....	25
19. Production history of well MT-31 .....	26
20. Production history of well MT-35 .....	26
21. Daily production rate and average enthalpy for Unit 1 wells .....	29
22. Daily production rate and average enthalpy for all production wells .....	30
23. Accumulated total, separated water and separated steam production from the Momotombo geothermal field .....	31
24. Pressure history of well MT-8 at 300 m b.s.l. ....	32
25. Pressure history of well MT-13 at 450 and 650 m b.s.l. ....	33
26. Enthalpy changes in wells MT-12 and MT-20 during discharge of well MT-9 .....	33
27. Density and dynamic viscosity ratios as a function of the saturation temperature ...	35
28. Ratio of steam and liquid water flowrates as a function of reservoir steam saturation .....	36
29. Relation between flowing enthalpy and mass fraction of steam in a reservoir .....	36
30. Wellhead enthalpy in 1991 as a function of depth to feedzones and estimated state of the shallow reservoir .....	38
31. Initial temperature distribution in Momotombo at 300 m b.s.l. ....	39
32. Volumes of water and steam in the shallow reservoir .....	41
33. Predicted cumulative production from the Momotombo geothermal field .....	42

## LIST OF TABLES

1. Overview of the Momotombo geothermal wells .....	19
2. Overview of the reinjection wells .....	27
3. Estimated production rates and enthalpies for second unit wells from March to September 1989 .....	31
4. Estimated depths to major feedzones of Momotombo production wells and dates of enthalpy increase .....	37
5. Percentage of initial fluid in storage withdrawn from the Momotombo reservoir ...	40

## 1. INTRODUCTION

This report presents the author's work during the last three months of the United Nations University (UNU) Geothermal Training Programme at the National Energy Authority in Reykjavik, Iceland. The author was carefully supervised by his adviser, Mr. Grimur Bjornsson throughout this time.

The main purpose of the programme was to provide the author with the necessary knowledge and experience in geothermal research and utilization for later use in his home country. The programme was divided into two parts. The first part consisted of lectures on the various aspects of geothermal research and utilization, field trips, and a week-long excursion in Iceland. In the second part, a detailed study was made on production data from the Momotombo geothermal field in Nicaragua.

### 1.1 Statement of the problem

The main objectives of the present study were:

- 1) To carry out a careful study of the measurement methods used to estimate total flowrates and enthalpies from Momotombo wells. This work included writing programs for a PC computer which solve mass flow equations for steam and water across orifices and weir boxes.
- 2) To collect and plot, with time, all available production data from the Momotombo geothermal wells.
- 3) To determine changes in the Momotombo reservoir due to exploitation over the last eight years (1983-1991), and make predictions of possible reservoir changes in the future.

### 1.2 Outline of the Momotombo geothermal field

The Momotombo geothermal field is located on the southern slope of the Momotombo volcano (Figure 1). The volcano has an elevation of 1250 m a.s.l., covers a surface area of 65 km<sup>2</sup> and is within the Momotombo - Galán volcanic complex (Martínez et al., 1988).

The geothermal field can be divided into two reservoirs located at different depths. The shallower one is liquid-dominated and is fed by the deeper one through active faults (González Solórzano, 1990). Most of the wells drilled, to date, intercept the shallow reservoir. Its characteristics are, therefore, much better known than those of the deeper reservoir.

The first generation of electricity by way of geothermal steam took place in Momotombo in September 1983, when a 35 MW<sub>e</sub> power plant began its production. A second unit came on-line in March 1989 with 35 MW<sub>e</sub> of installed capacity. Figure 2 shows the annual electricity production in Momotombo from 1983 up to the present time (Arcia Róger, personal communication, 1991). Relative to oil prices in 1989, the Momotombo geothermal field saved ten million US dollars that year (INE, 1989).

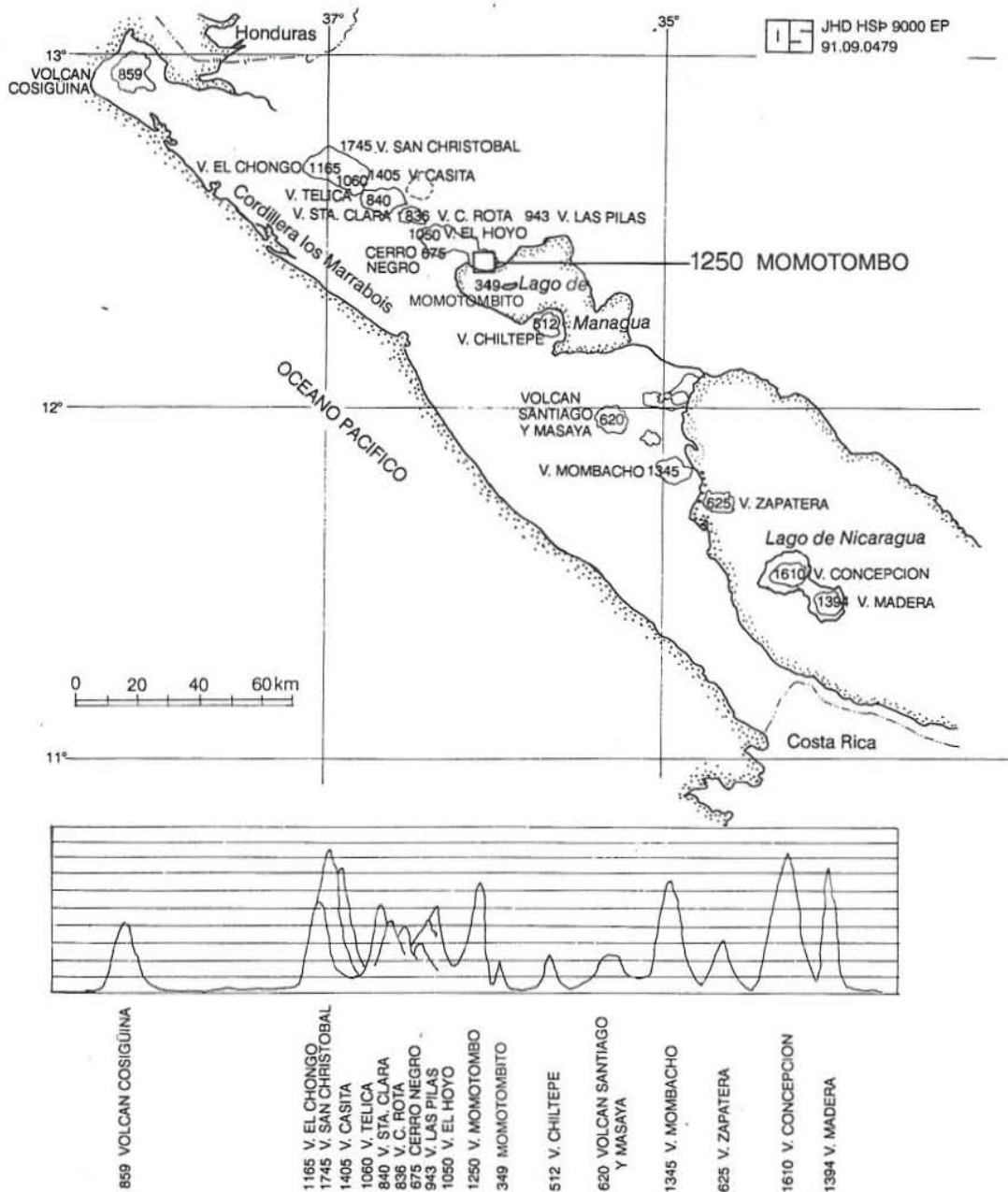


FIGURE 1: Location of the Momotombo geothermal field within the Cordillera Los Marrabios volcanic complex in Nicaragua (INE, 1989)

### 1.3 Data sources

The data used in the study was provided by División General de Recursos Geotérmicos of Instituto Nicaragüense de Energía (INE). Data on the fluid production from Momotombo for the first three years of production are scarce and of limited quality. But in November 1986, an effort was made to carefully monitor the production from the individual wells. Some reliable data is now available for most production wells for the period 1987 - 1991 (Kasap, 1986).

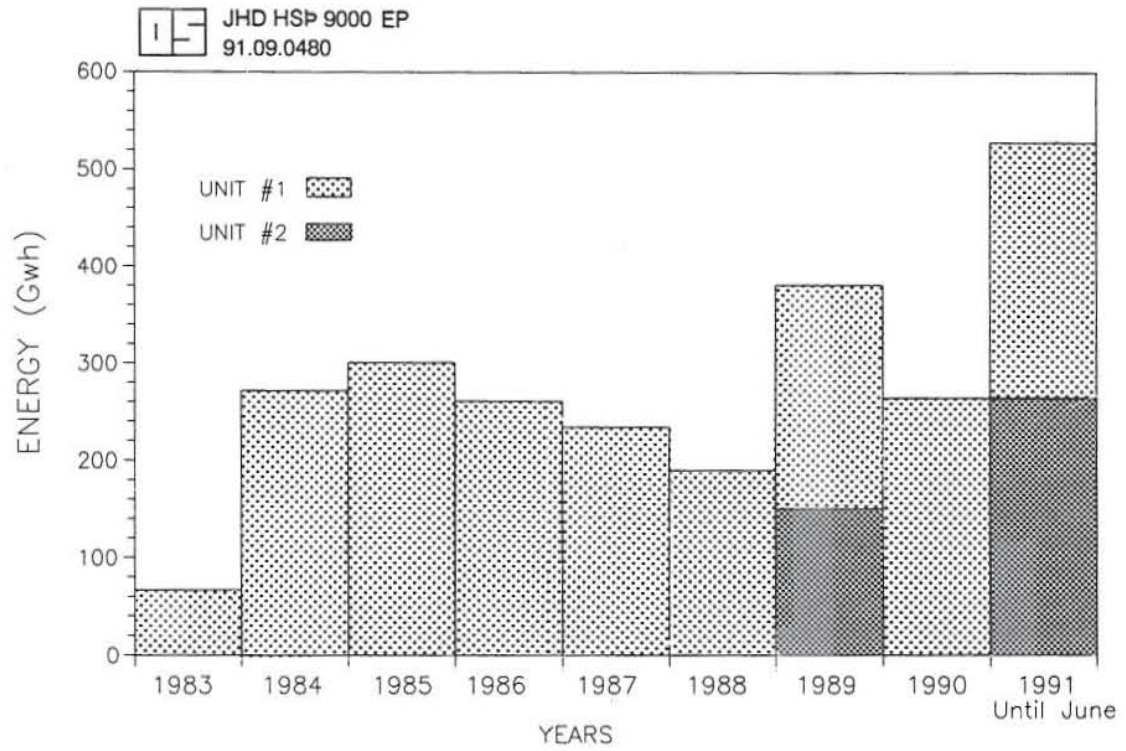


FIGURE 2: Annual electricity production of the two Momotombo units

## 2. DISCHARGE MEASUREMENTS OF TWO-PHASE WELLS

The monitoring of mass and energy flow from a geothermal well requires knowledge of parameters such as wellhead pressure, wellhead temperature, total flowrate and total enthalpy of the flow. These variables, in the case of a single-phase flow, are obtained for example by measuring the pressure drop over an orifice, or simply by measuring the time it takes to fill a container of known volume, whereas the enthalpy is given by the wellhead pressure and temperature. Things become more complicated if the well is producing a mixture of steam and water. In such a case, thermodynamic properties, such as the mass fraction of steam and wellhead pressure, are essential in order to determine the mass and energy output of a two-phase well.

In this chapter are discussed two common and well known methods of measuring two-phase flow from geothermal wells. They are:

- 1) The lip pressure method, sometimes called the Russel James method.
- 2) Separation of steam and water, and measuring the flowrates of the individual phases by conventional single-phase methods.

### 2.1 The lip pressure method

This method was proposed by Russel James (1970). It is based on a relationship observed between the flowing pressure at the end of a horizontal pipe which is discharging to the atmosphere and the enthalpy and the flowrate in the pipe (Figure 3). This pressure is called the lip pressure,  $P_{lip}$ , and is related to the total enthalpy  $h_t$  and the total flow per unit area in the pipe,  $G$ , (Grant et al., 1982) by:

$$\frac{Gh_t^{1.102}}{P_{lip}^{0.96}} = 1680 \quad (1)$$

In this equation  $P_{lip}$  is given in MPa,  $G$  in  $\text{kg}/\text{cm}^2/\text{s}$  and  $h_t$  in  $\text{kJ}/\text{kg}$ . Note that the equation is only valid if the flow is sonic at the end of the pipe. Equation 1 gives the product of the flowrate and the enthalpy. In order to know both parameters, the flow is separated after the pipe outlet and the flowrate of the  $100^\circ\text{C}$  liquid water,  $m_{la}$ , is measured in a weir box or by measuring the time it takes to fill a container of known volume.

The water flowrate is related to the total flowrate from the well,  $m_t$ , by mass and energy conservation, respectively

$$\begin{aligned} m_t &= m_{la} + m_{sa} \\ h_t &= x_a h_{sa} + (1 - x_a) h_{la} \end{aligned}$$

where the subscript  $a$  stands for atmospheric conditions,  $m_{sa}$  is the steam flowrate,  $x_a$  is the mass fraction of steam,  $h_t$  is the total enthalpy,  $h_{sa}$  and  $h_{la}$  are the enthalpies of steam and water respectively and  $m_{la}$  is the water flowrate given by equations described in Section 2.2.2.

Solving both equations for  $x_a$  gives

$$x_a = \frac{m_{sa}}{m_t} = \frac{m_t - m_{la}}{m_t} = \frac{h_t - h_{la}}{h_{sa} - h_{la}}$$



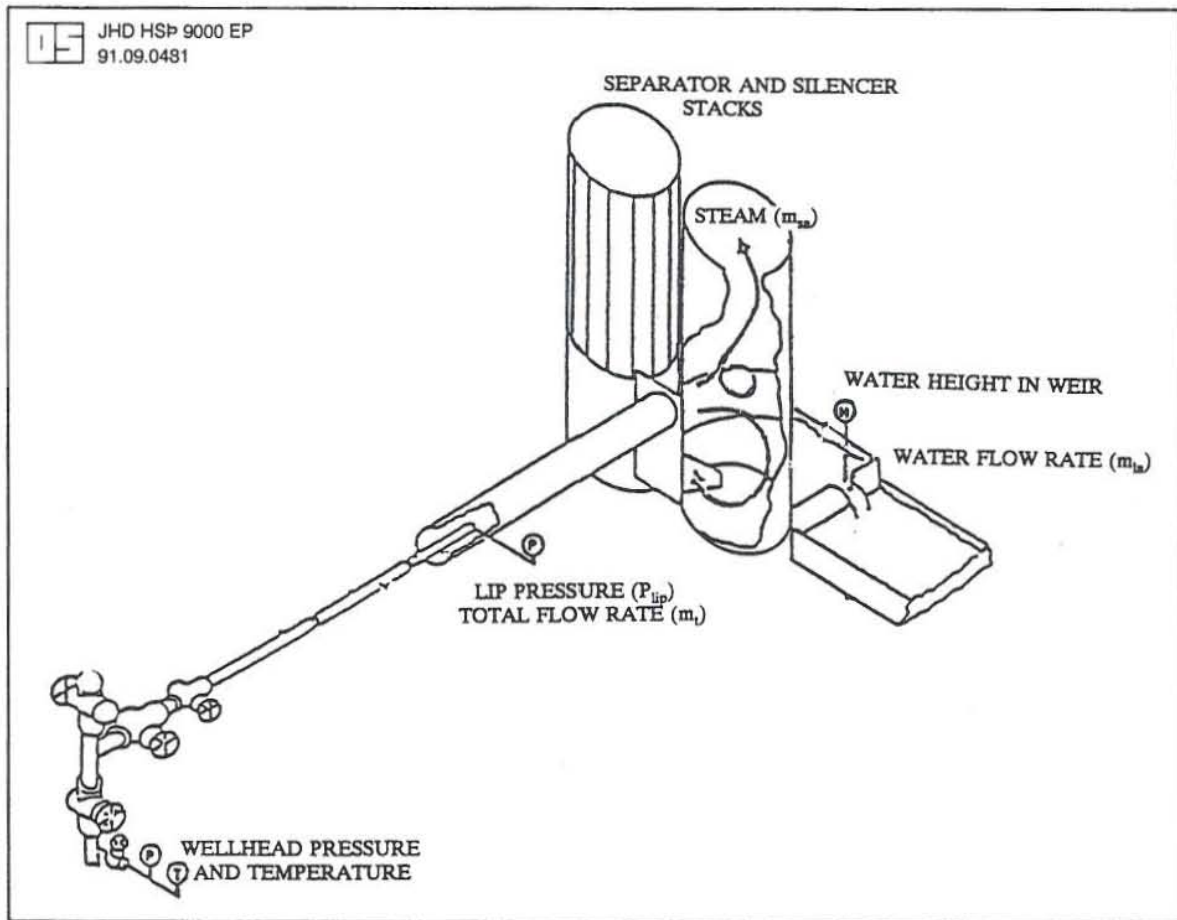


FIGURE 3: Typical wellhead equipment used to measure flowrate and enthalpy by the Russel James method

The total flowrate  $m_t$  equals  $m_{la}/(1 - x_d)$ . Inserting in Equation 1 and rearranging gives,

$$m_{la} = \frac{1680(h_{sa} - h_t)}{h_t^{1.102}(h_{sa} - h_{la})} A_d P_{lip}^{0.96} \quad (2)$$

where  $A_d$  is the cross-sectional area of the discharge pipe in  $\text{cm}^2$ .

The only unknown variable in Equation 2 is the total enthalpy  $h_t$ . Since the equation is non-linear, it has to be solved by iteration. A fortran program, LIP, was made for this purpose. The iteration algorithm used is the Newton iteration. By rewriting Equation 2, we want to find  $h_t$  such that

$$f(h_t) = m_{la} - \frac{1680(h_{sa} - h_t)}{h_t^{1.102}(h_{sa} - h_{la})} A_d P_{lip}^{0.96} = 0$$

If an initial guess for the enthalpy is  $h_i$ , a better solution  $h_{i+1}$  is given by

$$h_{i+1} = h_i - \frac{f(h_i)}{f'(h_i)} = h_i - \frac{f(h_i)\Delta h}{f(h_i + \Delta h) - f(h_i)}$$

This algorithm is repeated until  $f(h_i)$  becomes negligible (1 g/s).

When the enthalpy is known, the total flowrate  $m_t$  from the well is given by

$$m_t = \frac{m_{la}}{1-x_a} = \frac{m_{la}(h_{sa}-h_{la})}{(h_{sa}-h_t)} \quad (3)$$

A listing of the program LIP is given in Appendix I.

## 2.2 The steam separator method

The basic idea of this method is to separate the steam/water mixture from a geothermal well into two single-phase components using a typical cyclone separator (Figure 4). The flowrate of each phase is measured separately. The steam flow is generally measured by a pressure drop across an orifice plate, whereas the water flow is measured after it has flashed at atmospheric conditions.

### 2.2.1 Steam flowrate measurement

In this method, a pressure drop is induced by inserting an orifice into the steam flow line. As the steam passes the orifice, a significant pressure drop may occur, and this pressure drop is related to the flowrate by the following formulation (ASME, 1971). Assume we have a steady state, single-phase flow of an ideal compressible fluid across an orifice (Figure 5). The conservation laws of energy and mass before and after the orifice are then, respectively:

$$(u_{k_2} + u_{i_2}) - (u_{k_1} + u_{i_1}) = (p_1 v_1 - p_2 v_2) + (z_1 - z_2) + q_w \quad (4)$$

$$m = A_1 V_u \rho_1 = A_2 V_d \rho_2 \quad (5)$$

where  $u_k$  is the kinetic energy of the flow,  $u_i$  is the internal energy of the fluid,  $z$  is the elevation from a datum,  $V_u$  and  $V_d$  are the average velocities up and downstream, respectively,  $q_w$  is the heat transferred to or from the fluid,  $m$  is the flowrate in kg/s, and  $\rho$  is density. The subscript 1 and the area  $A_1$  refer to the upstream side of the orifice, whereas the subscript 2 and the area  $A_2$  denote the downstream side.

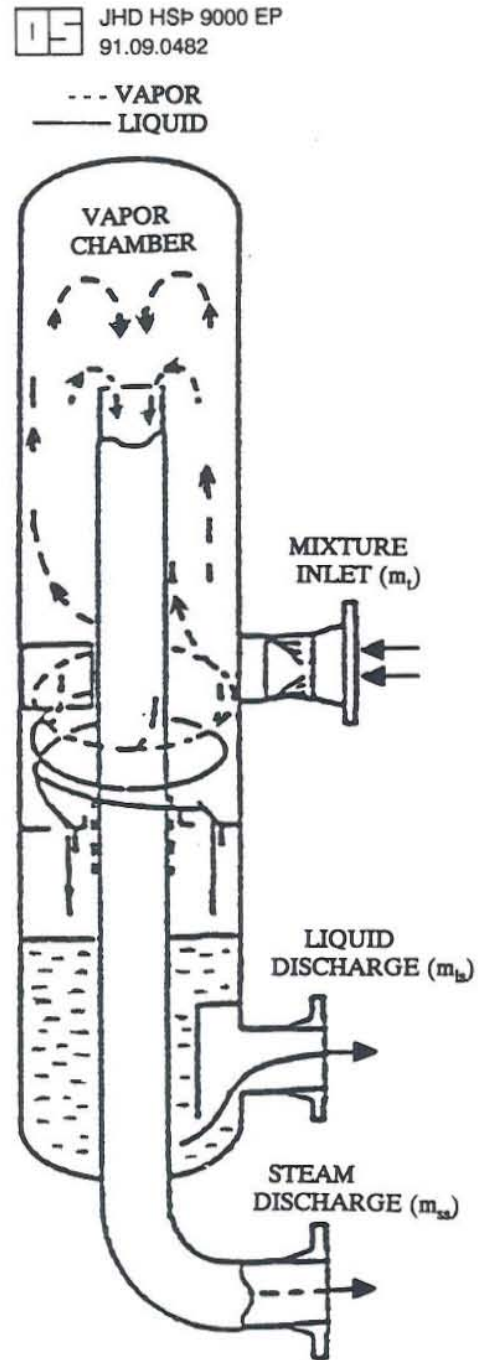


FIGURE 4: A sketch of a cyclone separator

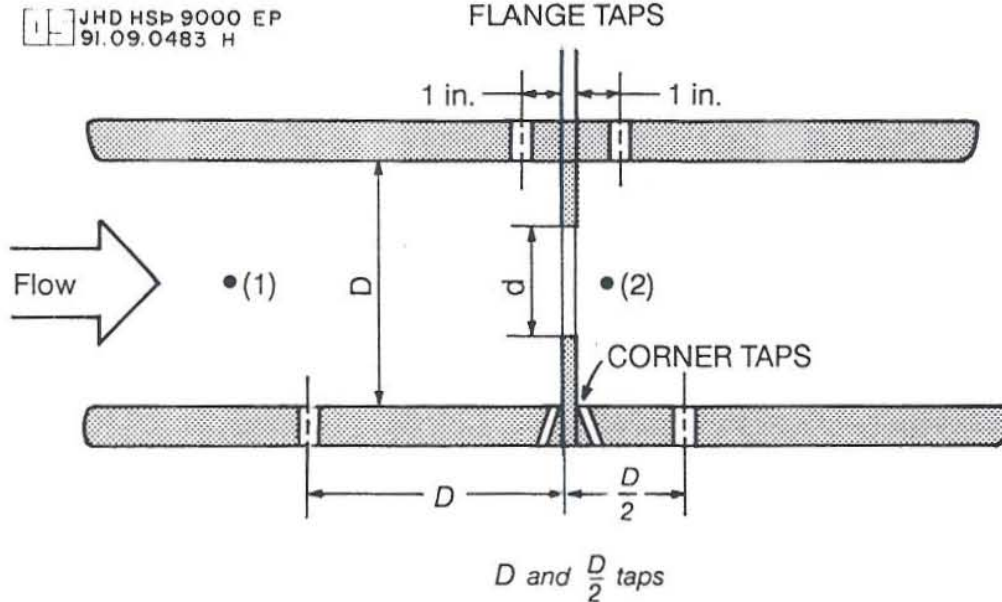


FIGURE 5: A sketch of a thin plate orifice in a flowline and the location of pressure taps (Fox and McDonald, 1985)

If we assume that no heat transfer takes place between the fluid and the pipe (no friction), then all changes of state between sections  $A_1$  and  $A_2$  are reversible and isentropic which gives

$$p_1 v_1^\gamma = p_2 v_2^\gamma = p v^\gamma = c \quad (6)$$

where  $\gamma$  is the ratio of the fluid specific heats and  $c$  is a constant.

In horizontal pipelines,  $z_1 = z_2$  which gives for Equation 4

$$\frac{V_d^2}{2g_c} - \frac{V_u^2}{2g_c} = h_1 - h_2 \quad (7)$$

where  $h = u_i + p v$  is the fluid enthalpy,  $g_c$  is a proportional constant and  $v$  is the specific volume of the fluid.

Also, for an ideal gas we have:

$$h_1 - h_2 = \int_{p_1}^{p_2} v dp$$

A solution to this integral is given in ASME (1971) and when inserted in Equation 7 we have

$$\frac{V_d^2}{2g_c} - \frac{V_u^2}{2g_c} = p_1 v_1 \left( \frac{\gamma}{\gamma-1} \right) \left( 1 - r^{\frac{\gamma-1}{\gamma}} \right) \quad (8)$$

where  $r = p_2/p_1$ .

Equations 5, 6 and 8 can now be combined into

$$V_d = \sqrt{\frac{\frac{2g_c p_1}{\rho_1} \left(\frac{\gamma}{\gamma-1}\right) (1-r)^{\frac{\gamma-1}{\gamma}}}{r - \left(\frac{A_2}{A_1}\right)^2 r^{\frac{2}{\gamma}}}}$$

Inserting  $V_d$  into Equation 5 gives the following desired solution for the flowrate in the pipe:

$$m = A_2 \sqrt{\frac{2g_c (p_1 - p_2) \rho_1 r^{\frac{2}{\gamma}} \left(\frac{\gamma}{\gamma-1}\right) \left(\frac{1-r}{1-r}\right)^{\frac{\gamma-1}{\gamma}}}{1 - \beta^4 r^{\frac{2}{\gamma}}}} \quad (9)$$

Equation 9 is called the theoretical adiabatic equation for the mass flowrate of an ideal compressible fluid across a section of area  $A_2$ .

By rearranging Equation 9 we get

$$m = A_2 Y \sqrt{\frac{2g_c \rho_1 (p_1 - p_2)}{1 - \beta^4}} \quad (10)$$

where  $Y$  is called the expansion factor of the fluid. This factor depends on  $r$ ,  $\gamma$  and the diameter ratio  $\beta = d/D$ , where  $D$  is the upstream diameter of the pipe and  $d$  is the downstream diameter.

Because most materials expand or contract as their temperature changes, a factor  $F_a$  must be introduced into Equation 10 in order to take into account any expansion changes of the area  $A_2$ . The factor  $F_a$  is, for example, 1.004 at 150° C for commercial steel.

In general, the real flowrate is less than the theoretical rate in Equation 10 as a result of previously stated assumptions. Hence, to obtain the actual flow from the theoretical equation, an additional discharge coefficient  $C_d$  is introduced (ASME, 1971):

$$m = \frac{\pi d^2 F_a C_d Y}{4\sqrt{1 - \beta^4}} \sqrt{2g_c \rho_1 (p_1 - p_2)} \quad (11)$$

If we, furthermore, define a flow coefficient  $\alpha$  as

$$\alpha = \frac{C_d}{\sqrt{1 - \beta^4}}$$

then Equation 11 can be written as

$$m = \frac{\pi}{4} d^2 F_a \alpha Y \sqrt{2g_c \rho_1 (p_1 - p_2)} \quad (12)$$

Defining  $\Delta p = p_1 - p_2$  and  $g_c = 9.80652$ , Equation 12 becomes (ASME, 1971):

$$m = 0.034783 \alpha Y \beta^2 D^2 F_a \sqrt{\rho_1 \Delta p} \quad (13)$$

Equation 13 is a general equation for steam flowrate through a thin plate orifice in a horizontal pipeline. In this equation the diameter must be in cm, the pressure in bars and the density in  $\text{kg/m}^3$  (ASME, 1971).

The discharge coefficient  $C_d$  is dependent on the location of the so-called pressure taps, which are located to either sides of the orifice. Several arrangements are used, among them flange taps, taps at  $1 D$  and  $0.5 D$ , vena contract and corner taps (Figure 5). Corner taps are used in the Momotombo steam-gathering system to measure steam flowrates. In these taps, the pressure holes open in the corner formed by the pipe wall and the orifice plate. The axial width of the openings should be  $0.02 D$ . The discharge coefficient for corner taps is given by the following empirical equation (White, 1979):

$$C_d \approx 0.5959 + 0.0312 \beta^{2.1} - 0.184 \beta^8 + 0.0029 \beta^{2.5} \left( \frac{10^6}{Re_D} \right)^{0.75} \quad (14)$$

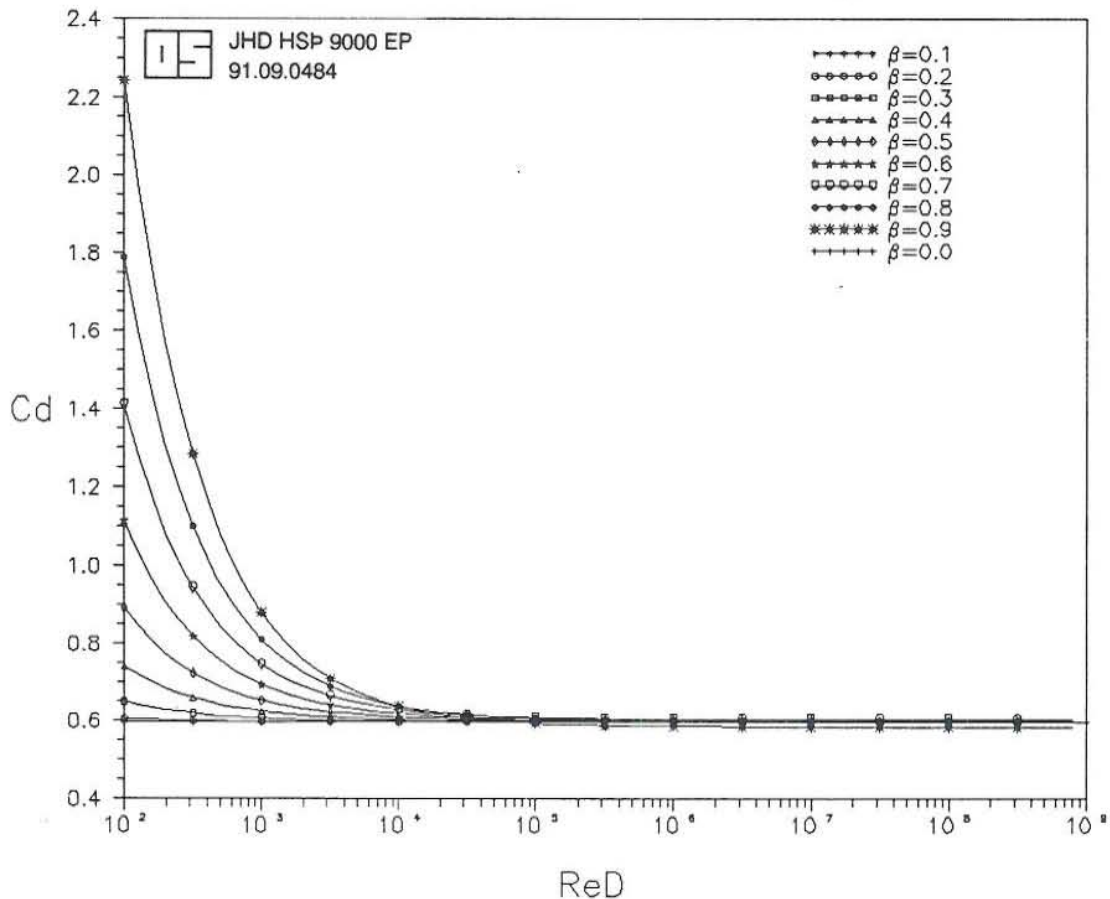


FIGURE 6: The discharge coefficient  $C_d$  for corner taps

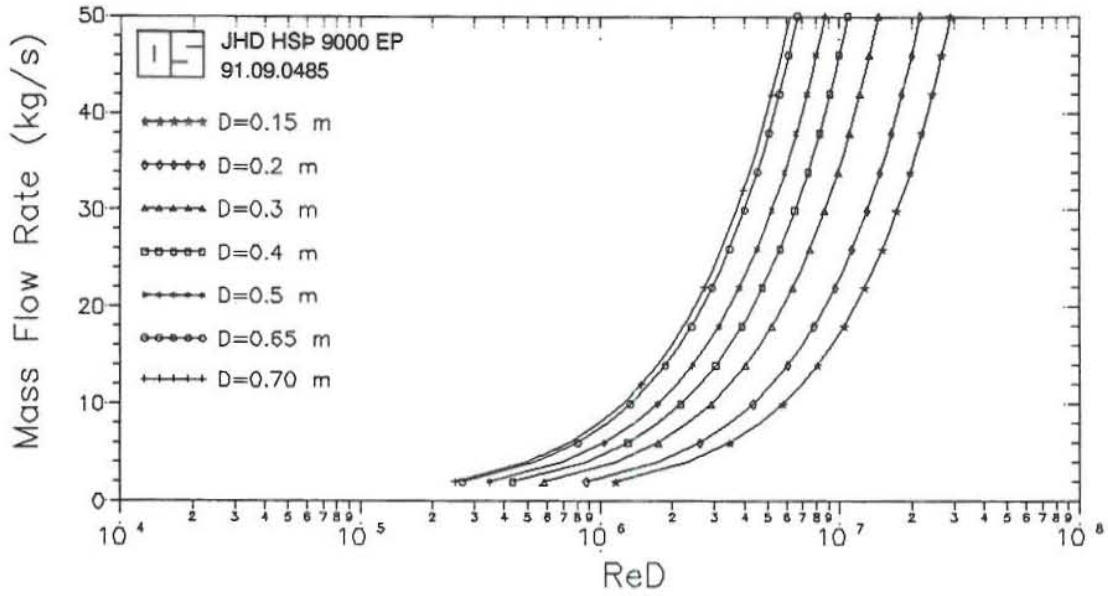


FIGURE 7: Reynolds number for different steam flowrates. The steam pressure is 8 bars-a

Figure 6 shows the value of  $C_d$  as a function of the Reynolds number for the flow and  $\beta$ . Figure 7, on the other hand, shows the Reynolds number for a single-phase steam flow as a function of flowrates and pipe diameters, but constant steam pressure 8 bar-a. The pipes used to transport steam from geothermal wells are generally of diameters ranging from 0.1 to 0.7 m. Figure 7 shows that typical Reynolds number for steam flow from geothermal wells are greater than  $10^5$ . This means that the last term of Equation 14 is negligible and, furthermore, that  $C_d$  is only dependent on  $\beta$ . This fact is also seen in Figure 6 where  $C_d$  becomes constant for  $Re_D > 10^5$ . Equation 14 is, therefore, approximated as

$$C_d \approx 0.5959 + 0.0312 \beta^{2.1} - 0.184 \beta^8$$

ASME (1971) also gives an empirical equation for  $Y$ , the expansion factor of steam, especially applicable to corner taps and steam velocities less than sonic. The relationship is

$$Y = 1 - (0.41 + 0.35 \beta^4) \frac{\Delta p}{P_1 \gamma}$$

where  $\gamma = 1.13$  for saturated steam at pressure 8 bars-a.

## 2.2.2 Water flowrate measurement

If the water from a cyclone separator is passed to a silencer and flashed to the atmosphere (Figure 3), the separated water flowrate is given as:

$$m_{is} = \frac{m_{ia}}{1 - x_a} = m_{ia} \frac{h_{sa} - h_{ia}}{h_{sa} - h_{is}} \quad (15)$$

where  $m_{is}$  is the water flow after the separator and  $m_{ia}$  is the water flowrate after atmospheric flashing. The  $h_{sa}$  and  $h_{ia}$  are, as before, the enthalpies for steam and water at the atmospheric

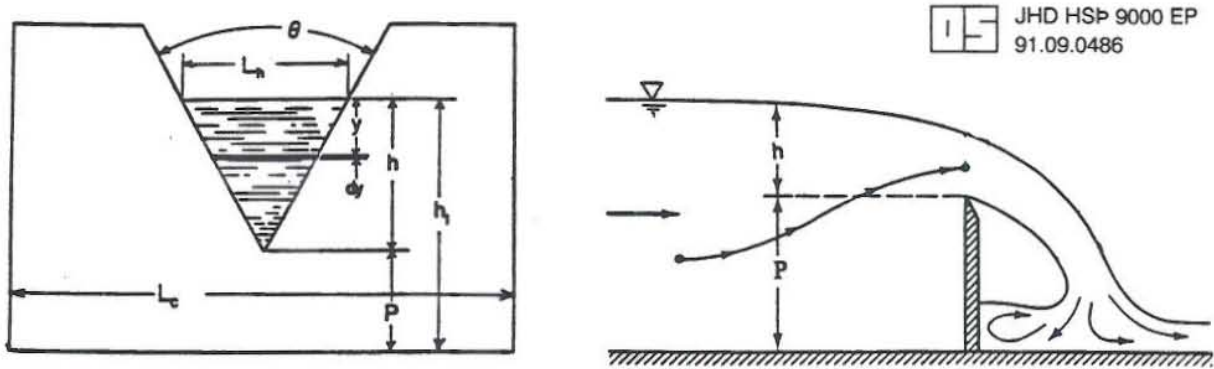


FIGURE 8: A sketch of a weir box (Modified after ASME, 1971 and White, 1979)

The calculation of  $m_{la}$  in Momotombo is based on flow measurements by weirs. A weir is an obstruction in the bottom of a channel which the flow must deflect over. For certain simple geometries the channel discharge  $m_{la}$  correlates with the blockage height to which the upstream flow is deflected by the presence of the weir. Many different types of weirs can be used, but the most common ones are the V-notch and the rectangular notch. V-notch weirs are used in Momotombo and a derivation of the flowrate across it is given by the following equations. Figure 8 shows a cross-section of a V-notch and its geometrical parameters. The theoretical velocity of a stream filament at a distance "y" below the water surface is:

$$V_s = \sqrt{2gy} \quad (16)$$

where  $g$  is the acceleration of gravity (ASME, 1971).

Then, the theoretical volumetric flowrate,  $dq$ , through the element segment  $dy$  is

$$dq = \sqrt{2gy} L_{h-y} dy \quad (17)$$

Integrating Equation 17 from  $y = 0$  to  $y = h$  gives

$$q = \frac{8}{15} C \tan \frac{\theta}{2} \sqrt{2gh^5} \quad (18)$$

where  $C$  is called the discharge coefficient for the V-notch.

When  $\theta = 90^\circ$  and  $g = 9.81 \text{ m/s}^2$  and multiplying Equation 18 by the fluid density, we get the following equation for the mass flowrate across a V-notch in kg/s:

$$m_{la} = \frac{8}{15} C \rho \sqrt{2gh^5} \quad (19)$$

The value of the discharge coefficient  $C$  is based on empirical data. A good assumption for its value is 0.585, given that 0.00085 m are added to the water height in the notch, and that the width of the weir box  $L_c$  is greater than  $2P$  and that  $h \leq P$  (ASME, 1971). This leads to a simple relationship between water height and flowrate in a  $90^\circ$  V-notch of the form

$$m_{la} = 1.38 \rho (h + 0.00085)^{2.5} \quad (20)$$

In our case of 100° C water from a silencer,  $\rho = 958 \text{ kg/m}^3$ .

### 2.2.3 Total enthalpy and flowrate from the well

Equations 13 and 20 give the steam flowrate  $m_{ss}$  from the separator and the water flowrate  $m_{la}$  after the silencer is applied. The total flowrate and enthalpy from the well are given as follows.

Assume that the liquid water from the separator flows adiabatically to the silencer and that the liquid enthalpy is the saturation enthalpy of water at the separator pressure  $P_s$ . By the conservation of mass and energy we have

$$h_{ls}(P_s) = x_a h_{sa}(P_a) + (1 - x_a) h_{la}(P_a)$$

or

$$x_a = \frac{h_{ls} - h_{la}}{h_{sa} - h_{la}}$$

The total flow  $m_{ls}$  discharged to the silencer is given as

$$m_{ls} = \frac{m_{la}}{1 - x_a} \quad (21)$$

The total flowrate from the well is then

$$m_t = m_{ls} + m_{ss} \quad (22)$$

which is readily defined by Equations 13 and 21.

The total enthalpy is, therefore,

$$h_t = \frac{m_{ss}}{m_t} h_{ss}(P_s) + \frac{m_{ls}}{m_t} h_{ls}(P_s) \quad (23)$$

A fortran program KASAP, was developed to solve the equations describing the flow of two single-phases of steam and water from the separator, where the water phase is flashed at atmospheric conditions. A listing of the program is given in Appendix I. The program uses the library STEAM (Bjarnason, 1985) to calculate the properties of steam and water on the saturation line. These routines are not listed in Appendix I.



### 3. PRODUCTION MONITORING IN THE MOMOTOMBO GEOTHERMAL FIELD

#### 3.1 Outline of the production history

Figure 9 shows the location of geothermal wells drilled so far in the Momotombo reservoir. Thirty-eight wells have been drilled of which twenty-two are productive, five are used for reinjection and eleven for monitoring. Table 1 gives an overview of these wells. Thirty-two wells were drilled between 1974-1978, twenty for production, eight for monitoring and four for reinjection. Additional drilling took place between 1982 and 1985. Six wells were drilled this time, one for reinjection, three for monitoring and two for production.

In September 1983, a 35 MW<sub>e</sub> power plant was installed in Momotombo (called Unit 1 Patricio Argüello Ryan). Five wells produced steam for the unit and four were connected to a reinjection system. Well MT-9 collapsed in 1988 and the electricity production declined for awhile. Two years later well MT-2 was on-line, replacing well MT-9.

A second unit of 35 MW<sub>e</sub> was installed in March, 1989. Six wells produced steam for this unit and the water from the separators of wells MT-35 and MT-36 was reinjected. Vibrations were detected in the second unit turbine after eight months of production and electricity production stopped until December, 1990. At this time, high quantities of non-condensable gases were detected from well MT-36. These gases reduced the efficiency of the turbine condenser drastically and the well had to be closed. In the near future, well MT-25 will be connected to the second unit, replacing well MT-36.

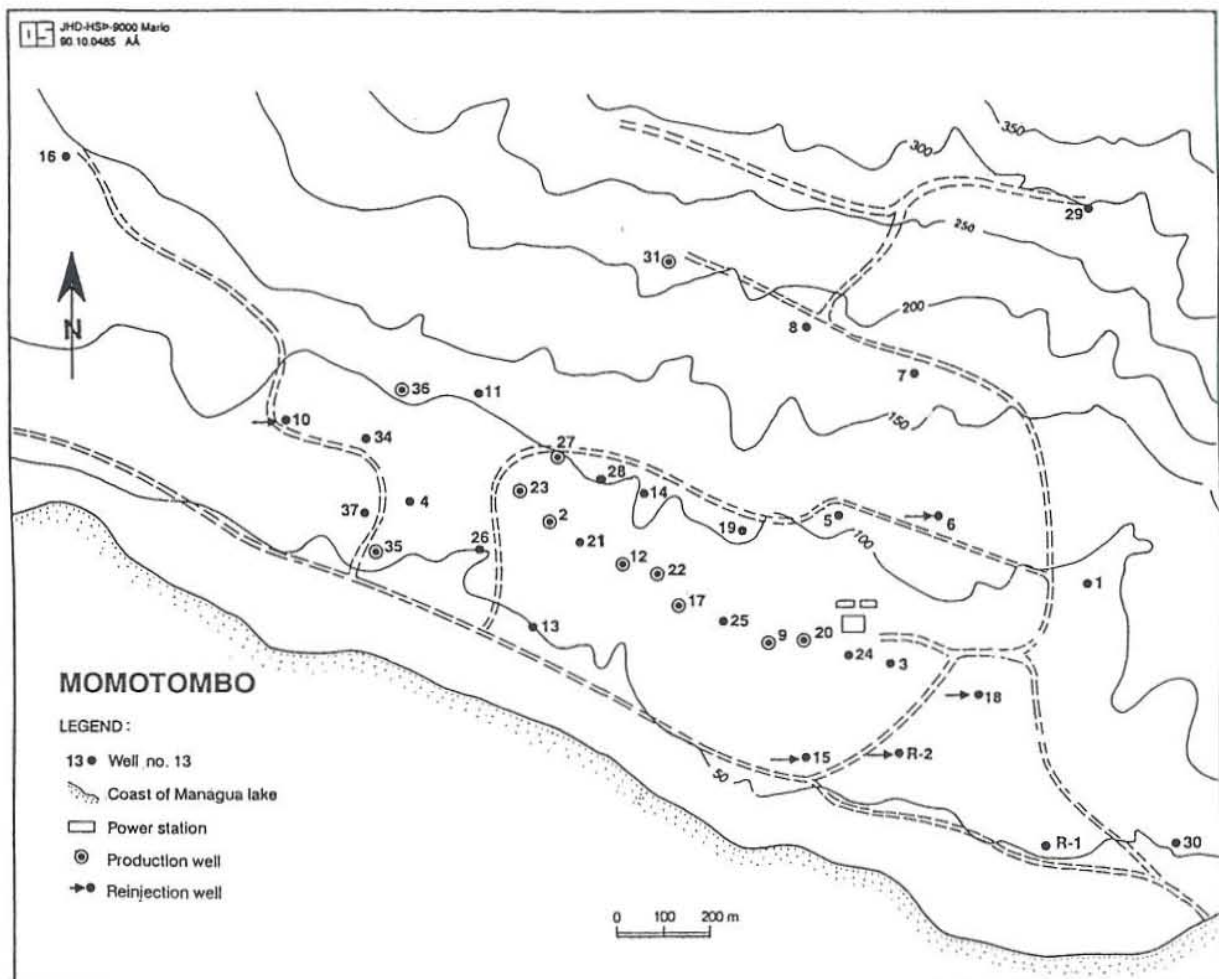


FIGURE 9: Areal map of the Momotombo geothermal field (González, 1990)

TABLE 1: Overview of the Momotombo geothermal wells

## MONITORING WELLS

Well Name	Depth (m)	Casing Depth (m)	Elevation (m)	Completion Time (dd,mm,yy)	Coordinate X (m)	Coordinate Y (m)
MT-1	1885	425	100	27-01-75	2567	642
RMT-1	1564	562	57	08-12-82	2115	15
MT-3	310	282	72	20-05-75 *	2122	44
MT-7	1798	595	175	01-03-76	2163	1082
MT-16	2251	827	106	14-03-77	50	1812
MT-29	944	481	289	23-03-78	2578	1492
MT-30	1852	369	58	17-05-78	2785	27
MT-34	985	516	86	30-05-83	923	925

## PRODUCTION WELLS

Well Name	Depth (m)	Casing Depth (m)	Elevation (m)	Completion Time (dd,mm,yy)	Coordinate X (m)	Coordinate Y (m)
†MT-2	488	366	60	06-05-75	1338	745
MT-4	1450	684	74	25-05-76	1023	787
MT-5	1124	377	105	01-12-75	2000	775
MT-8	1757	949	185	19-04-76	1913	1190
MT-9	616	232	80	29-05-76	549	1369
MT-11	1885	915	112	13-01-77	1180	1031
†MT-12	402	234	69	03-10-76	1504	655
MT-13	1824	260	49	18-12-76	1311	520
MT-14	670	243	101	03-11-76	1555	810
‡MT-17	328	285	71	10-06-77	1632	567
MT-19	536	259	98	30-07-77	1780	736
†MT-20	310	260	85	12-08-77	1922	490
MT-21	488	258	70	31-08-77	1413	702
‡MT-22	376	259	70	18-09-77	1582	635
†MT-23	821	260	68	09-10-77	1274	815
MT-24	455	250	83	27-10-77	2025	460
MT-25	455	253	73	22-11-77	1734	530
‡MT-26	638	365	49	15-12-77	1179	680
†MT-27	442	368	87	02-01-78	1365	896
MT-28	612	340	93	05-02-78	1458	840
‡MT-31	582	235	190	23-07-78	1602	1335
‡MT-35	1300	603	56	01-01-85	932	932
‡MT-36	1653	650	97	02-05-85	1002	1033
MT-37	1650		71		916	758

## REINJECTION WELLS

Well Name	Depth (m)	Casing Depth (m)	Elevation (m)	Completion Time (dd,mm,yy)	Coordinate X (m)	Coordinate Y (m)
RMT-2	1170	592	63	17-02-83	2146	235
MT-6	580	548	108	28-12-75	2228	784
MT-10	2104	760	99	14-08-76	730	960
MT-15	649	261	66	05-12-76	1936	220
MT-18	1124	256	74	10-07-77	2332	375

\* Initial date of drilling.

† Wells connected to the first unit.

‡ Wells connected to the second unit.

### 3.2 Production data from the individual wells

Considerable data are available on the mass and energy output from the individual Momotombo wells. The data were collected and given to the author by the staff of the División General de Recursos Geotérmicos (INE) in Managua, Nicaragua. The mass and energy flowrates were, in most cases, determined after the steam and liquid phases had been separated at the wellheads, and the flowrates of these two phases measured by methods described previously in Chapter 2. The steam flowrate measurements are nearly continuous in time for most production wells. The separated water flowrate, on the other hand, is discontinuous due to reinjection when water flowrate measurements are not possible.

**WELL MT-2:** This well was drilled in May 1975 down to 488 m depth and exploits fluid only from the shallow reservoir. It was connected to the power plant in June 1990. Figure 10 shows the production history of the well. The well produces an average of 25 kg/s at approximately 7 bars wellhead pressure and a total enthalpy of 2250 kJ/kg. The flowrate has been declining very rapidly since the first day of production. In the same way, the wellhead pressure and the separated water flowrate have been going down. The total enthalpy, on the other hand, has been increasing.

**WELL MT-9:** This well was drilled in May 1976 down to 616 m depth. It was connected to the power plant in 1983. Long term production data from this well are missing. Figure 11 shows the results of a production test conducted in 1988. It can be deduced from the figure that the well produced, as an average, 50 kg/s at 7 bars wellhead pressure and enthalpy of 1150 kJ/kg. The well collapsed in 1989, probably due to bad cementing of the production casing. Considerable interference has been observed between this well and wells in its vicinity. A more detailed description of this interference is given in Chapter 4.

**WELL MT-12** was drilled in October 1976. This well is 402 m deep and located at 67 m a.s.l. It was connected to the power plant in 1983. Figure 12 shows the production history of the well. The total flowrate was around 45 kg/s in January 1987, but has steadily decreased down to 20 kg/s

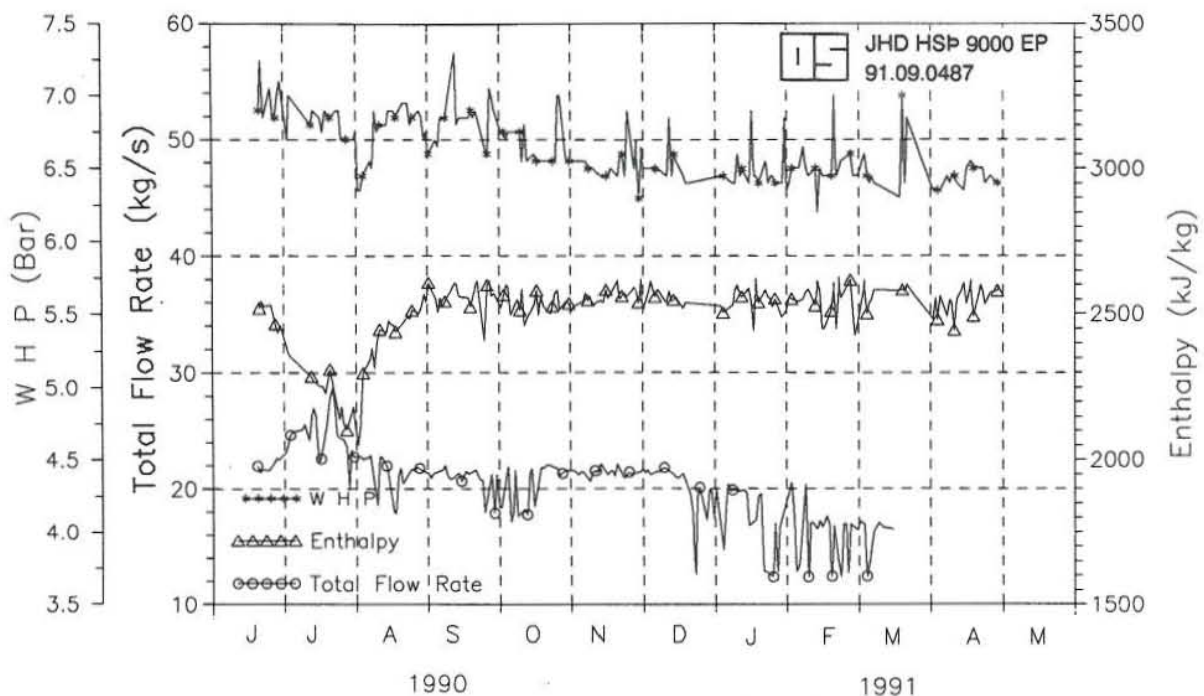


FIGURE 10: Production history of well MT-2

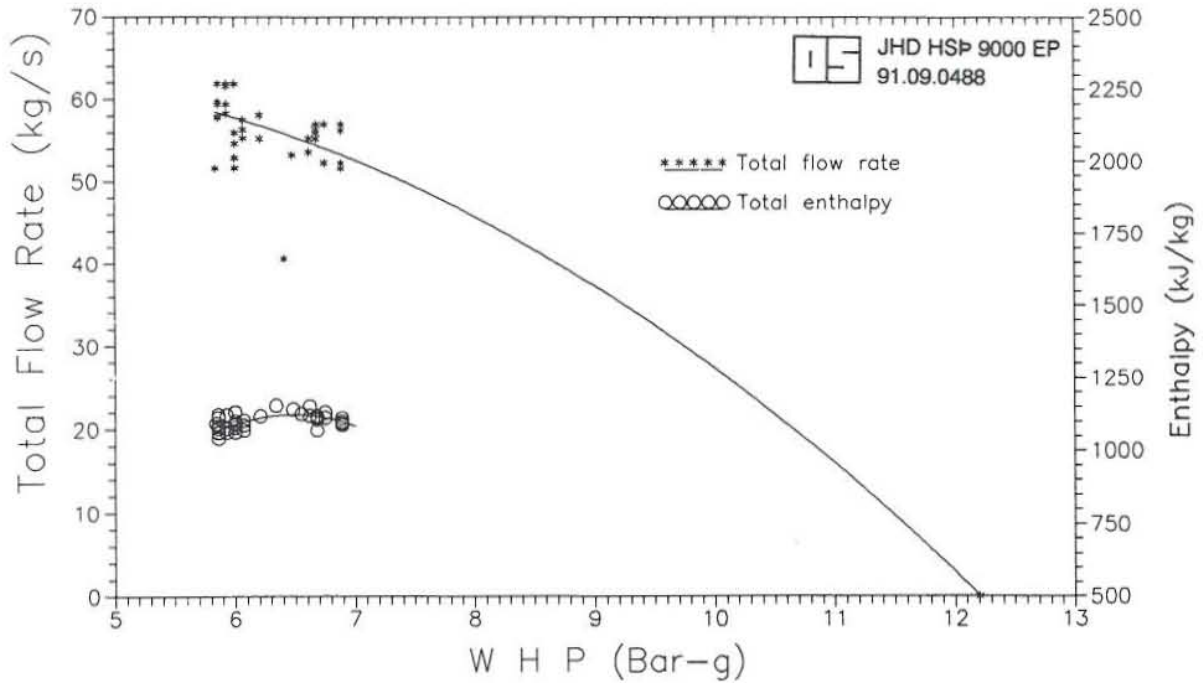


FIGURE 11: Output curve for well MT-9 in November 1988

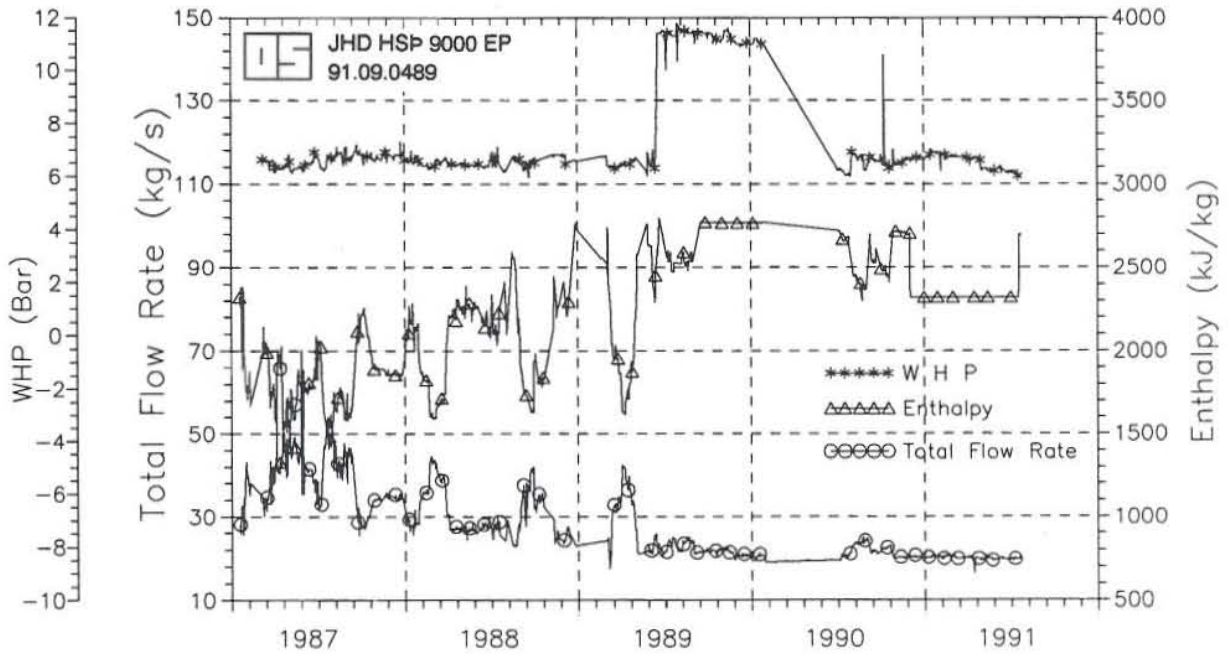


FIGURE 12: Production history of well MT-12

in 1991. The separated water flow from the wellhead has also decreased from 50 to 0 kg/s. The enthalpy, on the other hand, has increased from 1700 kJ/kg in 1987 to a dry steam enthalpy in 1991. The wellhead pressure and the steam flowrate have been nearly constant in time (6.6 bar and 20 kg/s), except in July 1989 when the wellhead pressure increased to almost 12 bars. Figure 12 also shows that the wellhead pressure has decreased since the second unit was replaced on-line in January 1991.

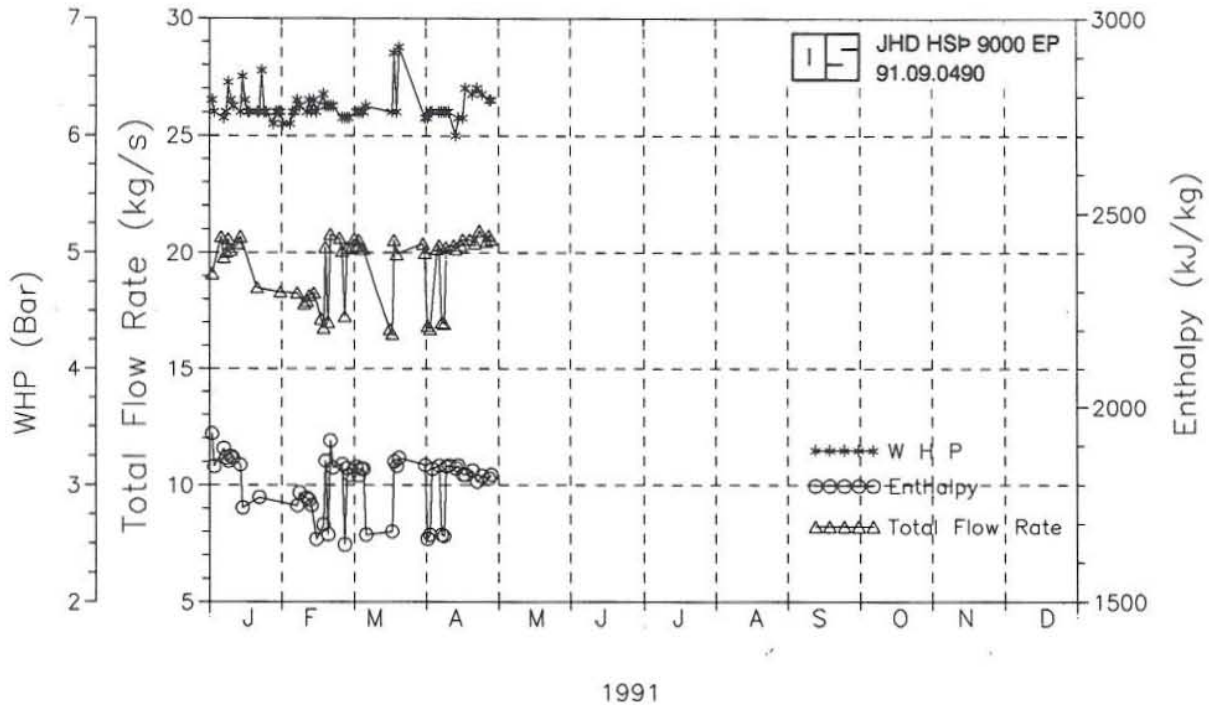


FIGURE 13: Production history of well MT-17

**WELL MT-17:** This well was drilled in June 1977. It is 328 m deep and located at 71 m a.s.l. Figure 13 shows the production data for the well since January 1991. The total flowrate is approximately 20 kg/s, the wellhead pressure has been nearly constant at 6.3 bars and the average enthalpy is around 1850 kJ/kg.

**WELL MT-20:** This well was drilled in August 1977. It is 310 m deep and located at 80 m a.s.l. It has been productive since 1983. Figure 14 shows the production data for the well. The total flowrate from the well has been unstable, especially before the second unit was installed in 1989. The wellhead pressure has changed in time in the same way as the total flowrate. The wellhead pressure has, as an example, declined by 0.5 bars between January and April 1991. These changes in the wellhead pressure and the total flowrate are coherent with production from wells in the vicinity of MT-20 (see Chapter 4). The wellhead temperature and, hence, the total enthalpy have increased since January 1989. The separated water flowrate was around 12 kg/s during 1987 and 1988, but in early 1989 the well went totally dry.

**WELL MT-22:** It was drilled in September 1977. This well is 376 m deep and located at 70 m a.s.l. Its production history is given in Figure 15. The total flowrate has been around 27 kg/s for the short production period shown. The separated steam and water flowrates are, on the average, 9 and 19 kg/s, respectively, and the total enthalpy is around 1375 kJ/kg.

**WELL MT-23:** This well was drilled in October 1977. It is 821 m deep, located at 71 m a.s.l. The production history of the well is shown in Figure 16. The figure shows clearly how the total flowrate has declined from 60 kg/s in 1987 to 40 kg/s in 1991. This decline rate has increased since the second unit was connected. In the same way, the separated water flowrate decreased from 49 to around 30 kg/s after four years of production (1987 - 1991). The steam flowrate, on the other hand, has been nearly constant over time (10 kg/s), until 1991 when it began to decline. The

produced enthalpy was constant from 1987 to 1989, but has increased since 1989. A good average of the enthalpy could be 1200 kJ/kg from January to April 1991. The wellhead pressure was around 6.6 bars between 1987 and 1990, but a small decline took place after January 1991.

**WELL MT-26:** This well was drilled in December 1977. It is 638 m deep and located at 49 m a.s.l. The production history of the well is shown in Figure 17. The total flowrate from this well has increased from 52 to 57 kg/s since January 1991. The separated steam flowrate is presently around

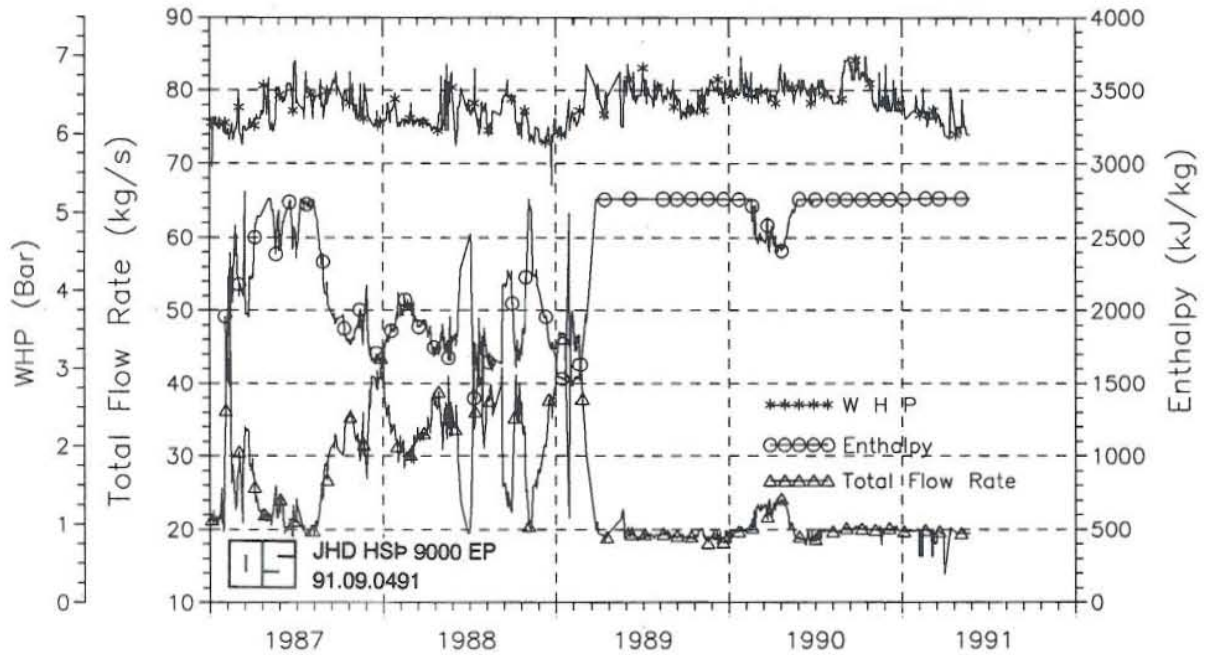


FIGURE 14: Production history of well MT-20

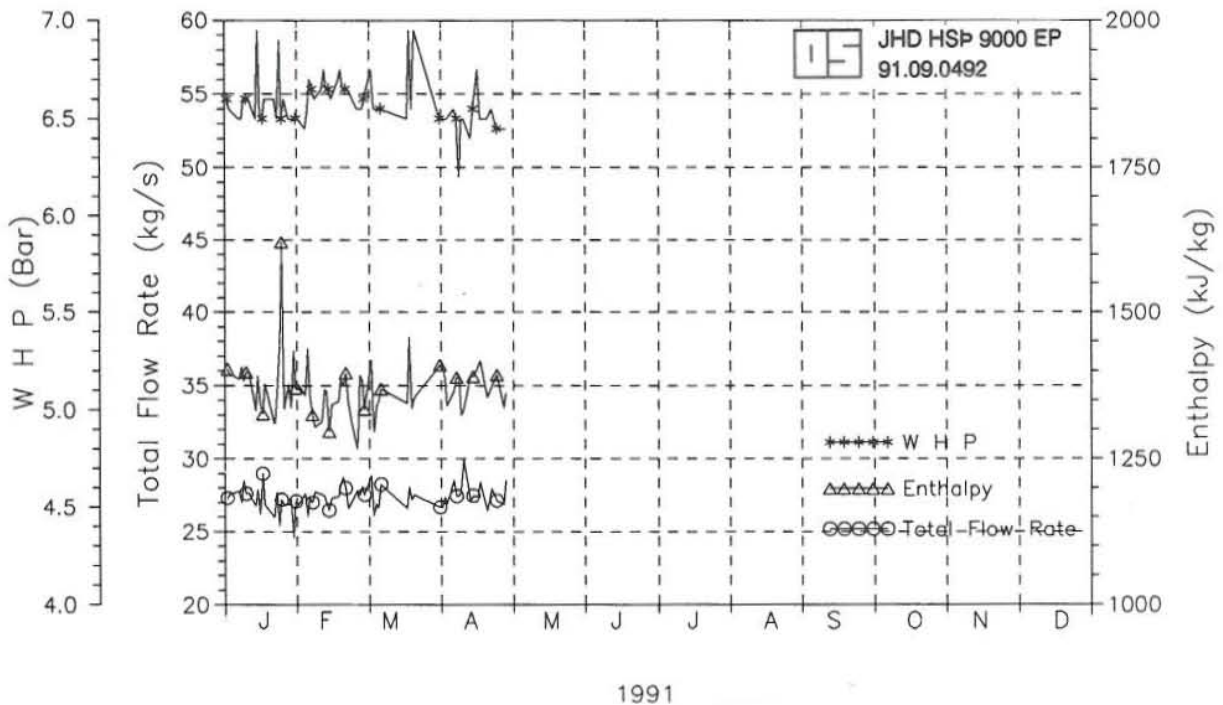


FIGURE 15: Production history of well MT-22

10 kg/s and the water flowrate around 47 kg/s. A small decline in the separated water flowrate can be seen from January until today. The wellhead pressure and temperature have been constant in time at around 6.3 bars and 168°C, respectively, since January 1991. A good average for the total enthalpy is 1055 kJ/kg.

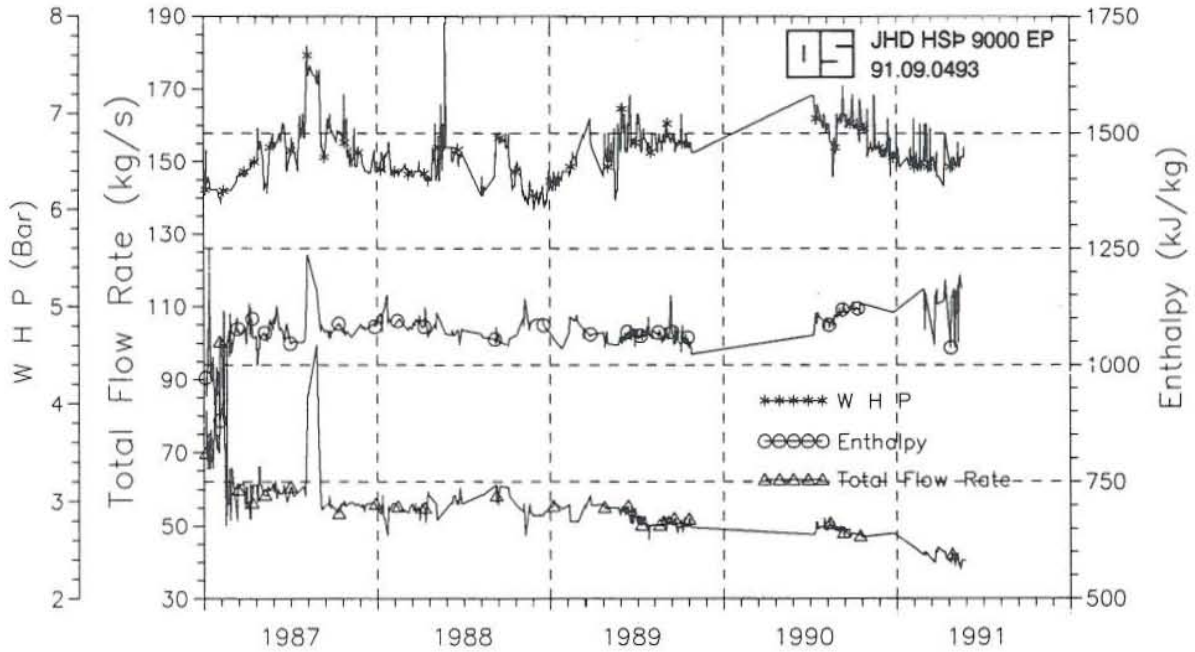


FIGURE 16: Production history of well MT-23

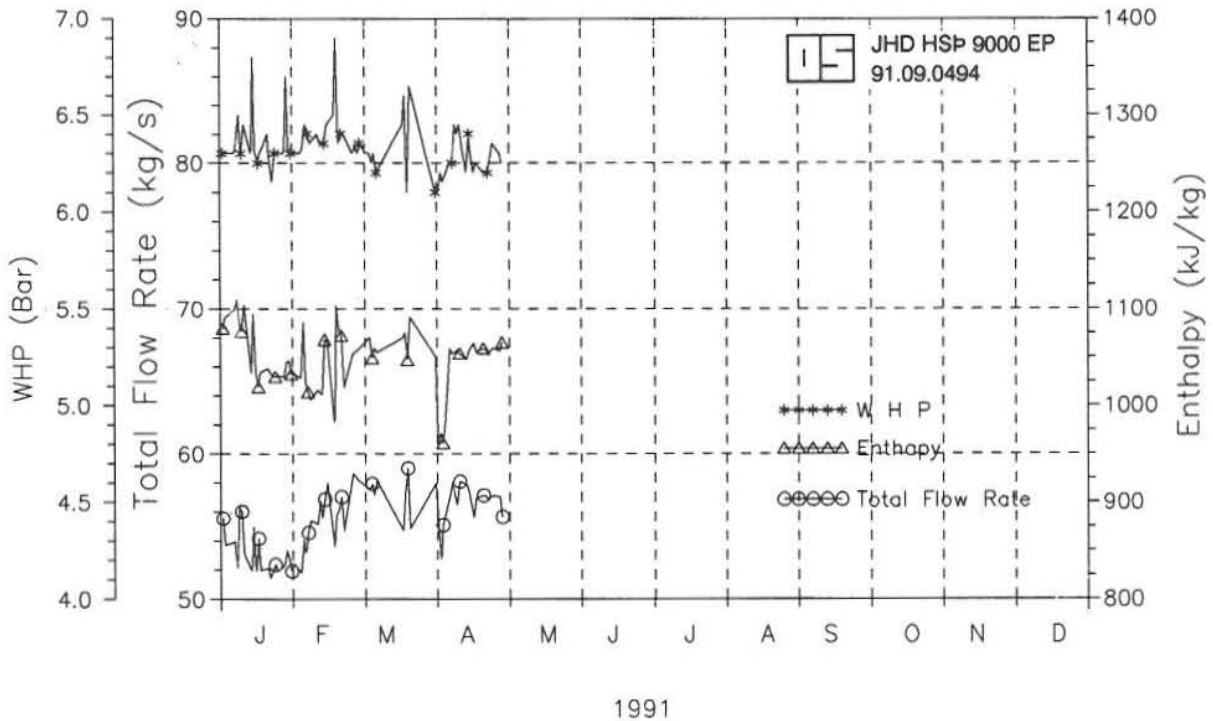


FIGURE 17: Production history of well MT-26

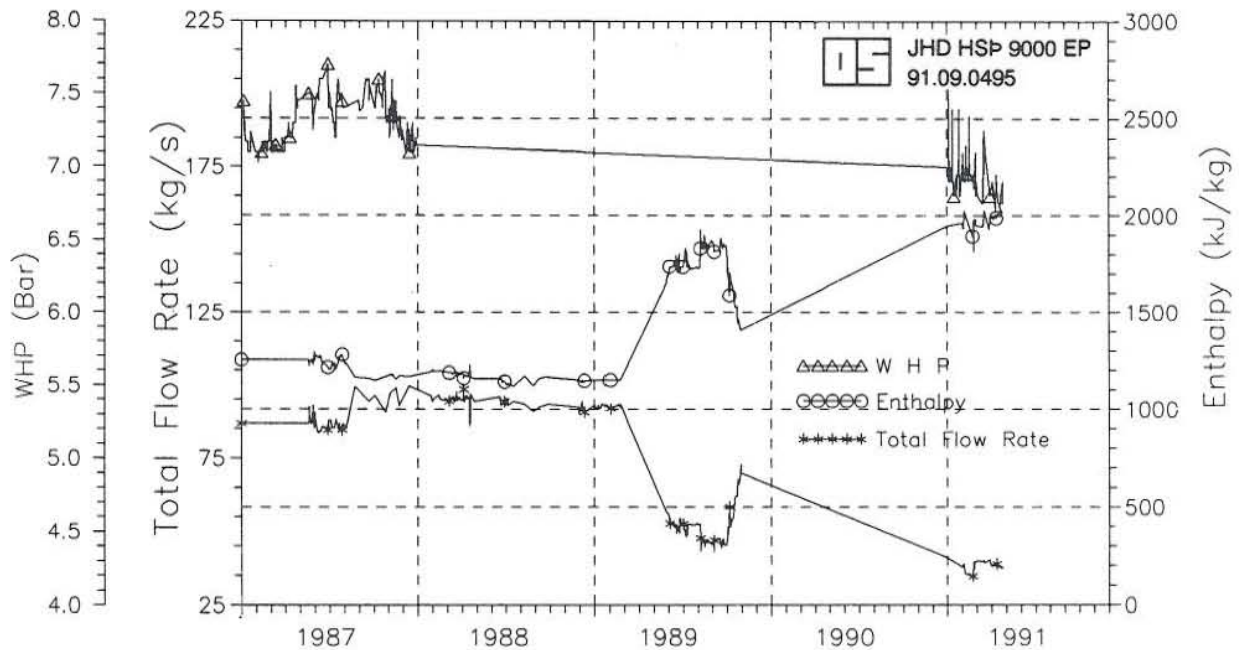


FIGURE 18: Production history of well MT-27

**WELL MT-27:** This well was drilled in January 1978 down to 442 m depth. Its production history is shown in Figure 18. The total flowrate was around 100 kg/s from January 1987 to March 1989, when it declined down to 35 kg/s due to increased production when Unit 2 came on-line. The steam flowrate has been around 23 kg/s since 1987, but the water flowrate has declined rapidly, which is reflected in higher total enthalpy. Production data from this well are missing from November 1989 to December 1990. Figure 18 also shows a decline in the wellhead pressure since 1987, especially since January 1991 when Unit 2 was replaced on-line.

**WELL MT-31:** This well was drilled in August 1978. It is 582 m deep and located at 201 m a.s.l. Figure 19 shows the production history of the well. The figure shows clearly how the total flowrate has declined in time; the slope is about 1.5 kg/s for the four months of production shown. The well became a dry steam well from its first day of production. The wellhead pressure and temperature have increased around 0.5 bars and 9°C, respectively, since January 1991.

**WELL MT-35:** This well was drilled in January 1985, down to 1300 m depth and is the first production well in Momotombo which produces directly from the deeper reservoir. The production history of the well is given in Figure 20. The total flowrate has declined from 57 to 39 kg/s after only four months of production. The steam flowrate has also declined from 30 to 20 kg/s. The wellhead pressure has been constant at 6.2 bars and the enthalpy is, on the average, 1720 kJ/kg.

**WELL MT-36:** This well was drilled in May 1985. It is 1653 m deep and located at 97 m a.s.l. This is the second well in Momotombo which produces fluid from the deeper reservoir. No production data is available from this well but an INE report (1989) gives some initial production data for the well. The total flowrate is given around 25 kg/s, whereof 17 kg/s are steam; the enthalpy is around 2200 kJ/kg. High quantities of non-condensable gases are observed in the well. They may be of volcanic origin (Recursos Geotérmicos - INE). These non-condensable gases reduced the efficiency of the turbine condenser and the well had to be closed.



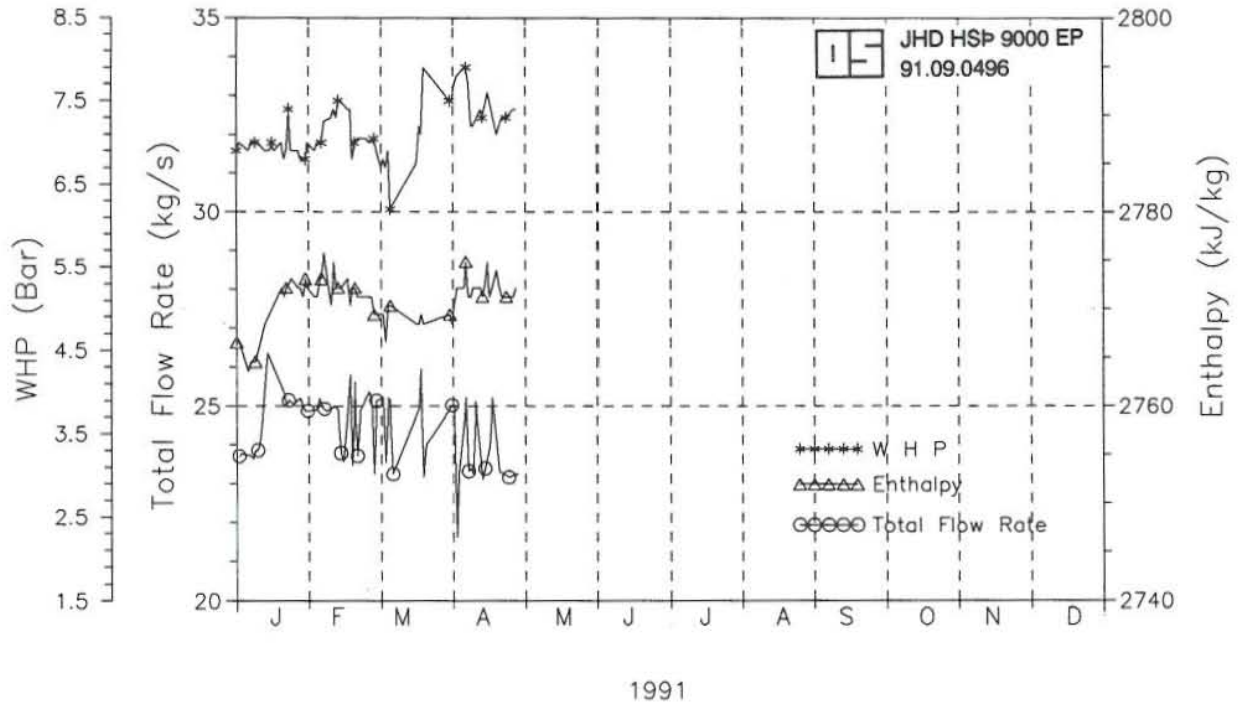


FIGURE 19: Production history of well MT-31

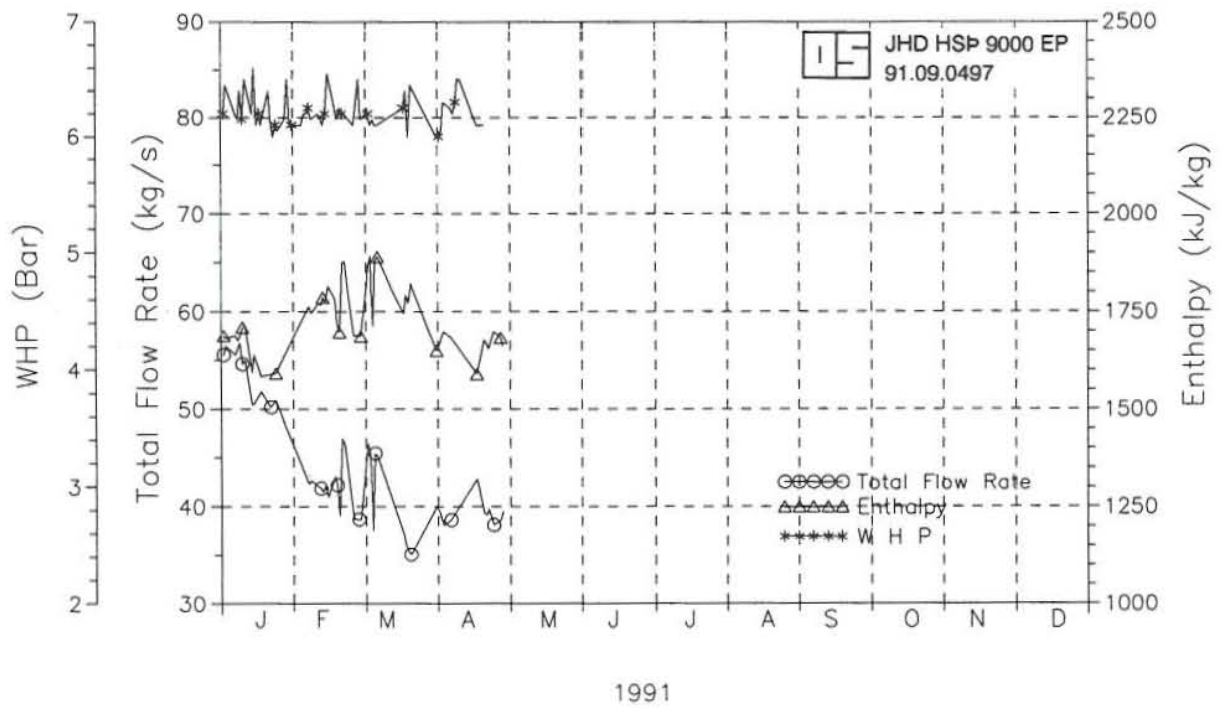


FIGURE 20: Production history of well MT-35

### 3.3 Reinjection data

Intensive mass production from a geothermal reservoir may result in a significant pressure drawdown and reduced flowrates from the production wells. It is possible to delay or even prevent this problem by reinjecting the excess water from the separators. This counts especially for low enthalpy reservoirs such as Momotombo where high volumes of fluid are extracted. The reinjected fluid will maintain the reservoir pressure and extend the productive life of the reservoir. The reinjection can also be used for sending polluted water back to its origin. But on the other hand, it might create cooling and scaling in wells and in the reservoir.

A reinjection system has been operating in Momotombo since 1983. The reinjected fluid has been separated water from five production wells (MT-23, MT-27, MT-31, MT-35 and MT-36). Approximately 80 % of the total water from the separators of these five production wells is reinjected back into the reservoir. The separated water is either passed to a pressurized pumping system which collects water from three of the production wells, or is piped directly from the separators into reinjection wells. Table 2 gives an overview of the reinjection process. Data on injection rates are missing from the study.

TABLE 2: Overview of the reinjection wells in Momotombo

Well	Main feedzones (m)	Injection period (years)	Type of injection
RMT-2	1094 - 1170 *	Since 1983	Pumping system
MT-6	300 - 400 *	1983 - 1988 1989 - 1990	Pumping system By gravity from MT-31
MT-10	400 - 700 *	1989 - 1990	By gravity from MT-36
MT-15	300 - 400 *	Since 1983	Pumping system
MT-18	700 - 800 *	Since 1983	Pumping system

\* Depths to feedzones are taken from Girelli et al. (1977) and González Solórzano (1990).

#### 4. ANALYSIS ON THE PRODUCTION DATA

The production data presented in Chapter 3 show some considerable changes in mass and energy flowrates for most of the wells considered. It is of interest to know if these changes are only due to a change of state in the reservoir close to the productive wells, or if the production has induced widespread changes in the reservoir which may have some serious consequences on the future performance of the field. This kind of analysis requires information on the total production, reservoir pressure, permeability and the extent of boiling in the reservoir.

##### 4.1 Daily and cumulative production

In order to analyze the areal extent of reservoir changes due to production, a compilation of the daily production was performed. Two fortran programs were developed for this purpose, called MOM and CUM (Appendix I). The latter one calculates the separated flowrates of steam and water and the total enthalpy for a production well for every day since January 1<sup>st</sup>, 1987. As data were not available for every day of the year, a linear extrapolation was used between days of measurements. This daily production data was written to files for each production well. The program CUM calculates the cumulative production of the separated steam and water phases using the MOM output files as an input. The program was also used to calculate total flowrates from the wells on a daily basis and the average enthalpy of the fluid produced (weighed by the flowrate for each well). The results are shown in Figures 21-23.

Figure 21 shows daily production rates for wells which have produced into the first unit of the Momotombo Power Plant. These wells have been monitored regularly since 1987 and, therefore, show a continuous record of the state of the fluid withdrawn from the reservoir. The figure shows relatively stable flowrates of separated steam and water until 1989, when a sudden drop in water flowrate is observed. This change occurs shortly after Unit 2 starts production and steam flow from the field is doubled. Unit 2 had to be switched off in October 1989 and, consequently, the mass production returned to its previous state. A small recovery follows in the total water flowrate from Unit 1 wells, but only for a few months. From there, a steady decline in total and water flowrates is seen, and hence, an increase in steam fraction and enthalpy. It should be noted that production data for well MT-9 are missing in Figure 21, and also that a step increase in flowrates in June 1990 follows the discharge of well MT-2.

Figure 22 shows daily flowrates for all production wells in Momotombo (Unit 1 and Unit 2). The data in this figure are incomplete due to the lack of production measurements for Unit 2 wells in 1989. Estimated constant values, based upon the production data from 1991 are, therefore, used for the 1989 production. Table 3 gives the estimated values used. As in Figure 21, it is obvious that the 1989 increase in production resulted in a dramatic change in the state of the produced fluid, reflecting a widespread change in the reservoir conditions.

Figure 23 shows cumulative production of steam, water and total mass from all production wells for the period 1983-1991. Production rates for the years 1983-1986 were not available for the study, and are estimated. The stable flowrates from 1987-1988 in Figure 21, indicate an almost constant production of approximately 95 kg/s of separated steam and 170 kg/s of separated water at a constant enthalpy of 1130 kJ/kg. This assumption is, furthermore, supported by the almost stable 35 MW<sub>e</sub> generation during 1983-1988 (Figure 2). Figure 23 shows that over 60 million tons of fluid have been produced from the Momotombo reservoir. The figure also clearly shows the permanent change in reservoir conditions which took place in 1989, when the separated water flowrate began to decline and the enthalpy increased.

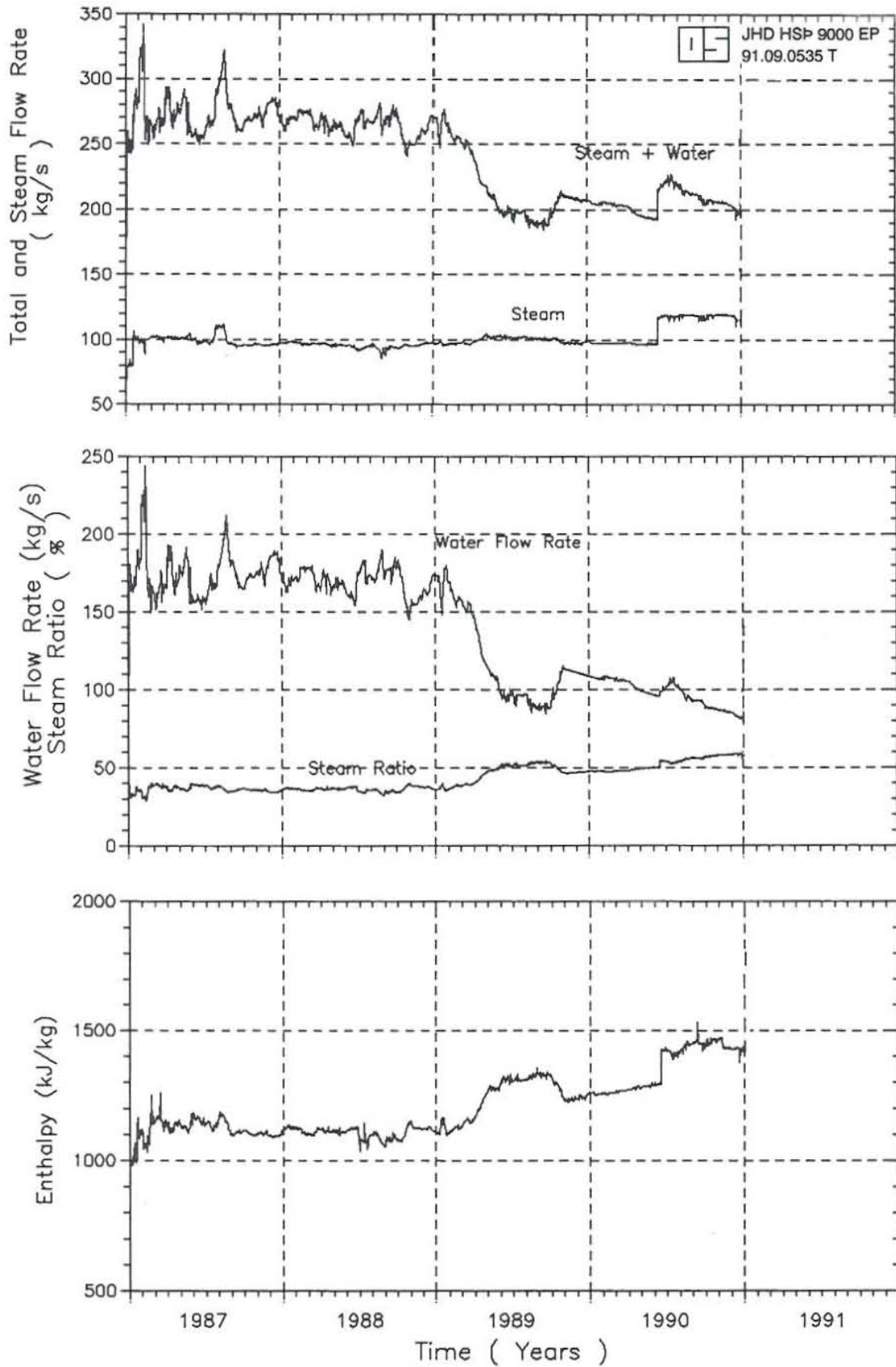


FIGURE 21: Daily production rates and average enthalpy for Unit 1 wells

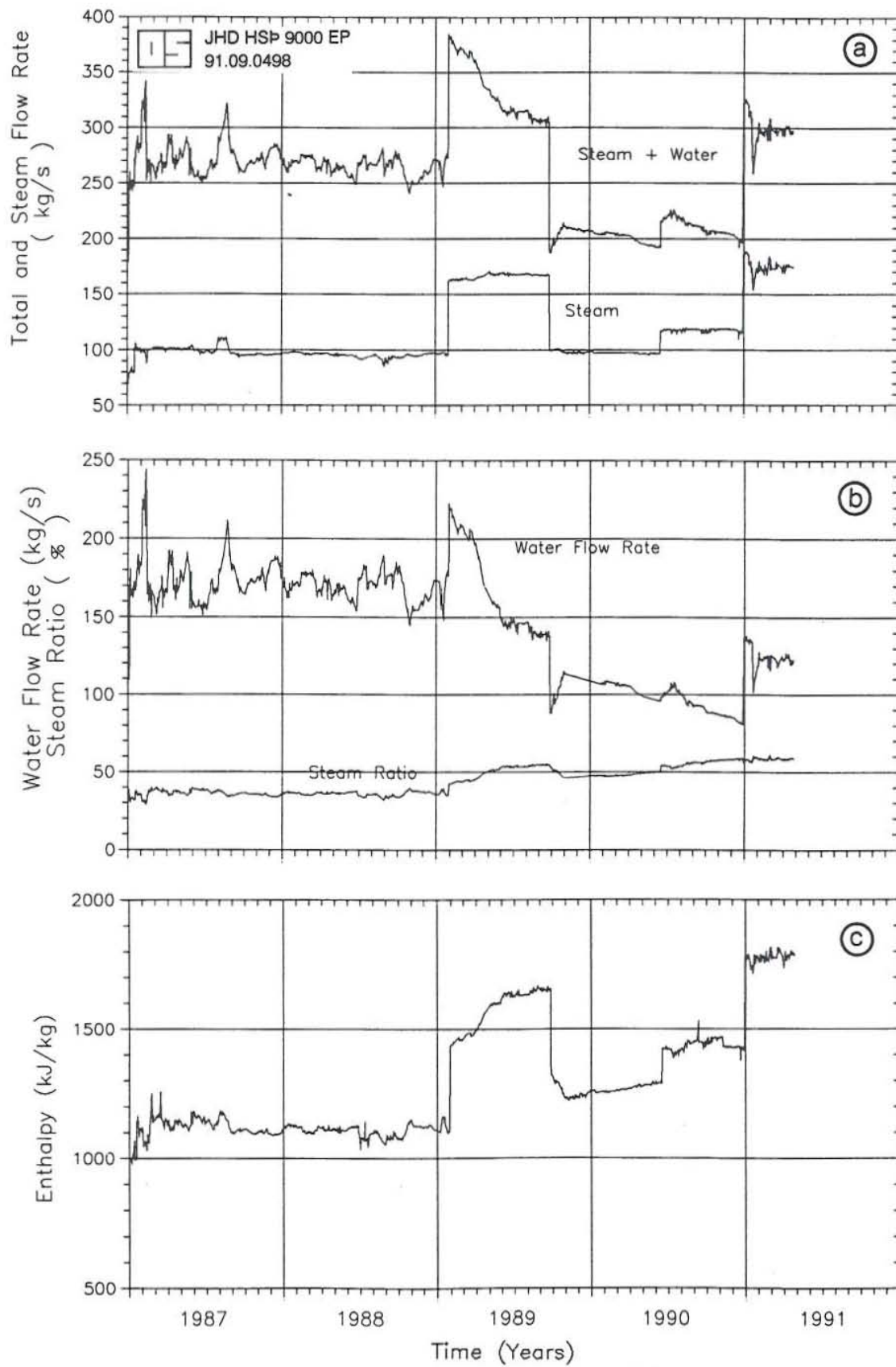


FIGURE 22: Daily production rates and average enthalpy for all production wells

TABLE 3: Estimated production rates and enthalpies for second unit wells from March to September 1989

Well number	Steam flowrate (kg/s)	Water flowrate (kg/s)	Total enthalpy (kJ/kg)
MT-17	11.5	9.5	1830
MT-22	9	18.5	1350
MT-26	9	19	1359
MT-31	24	0	2770
MT-35	22	22	1700

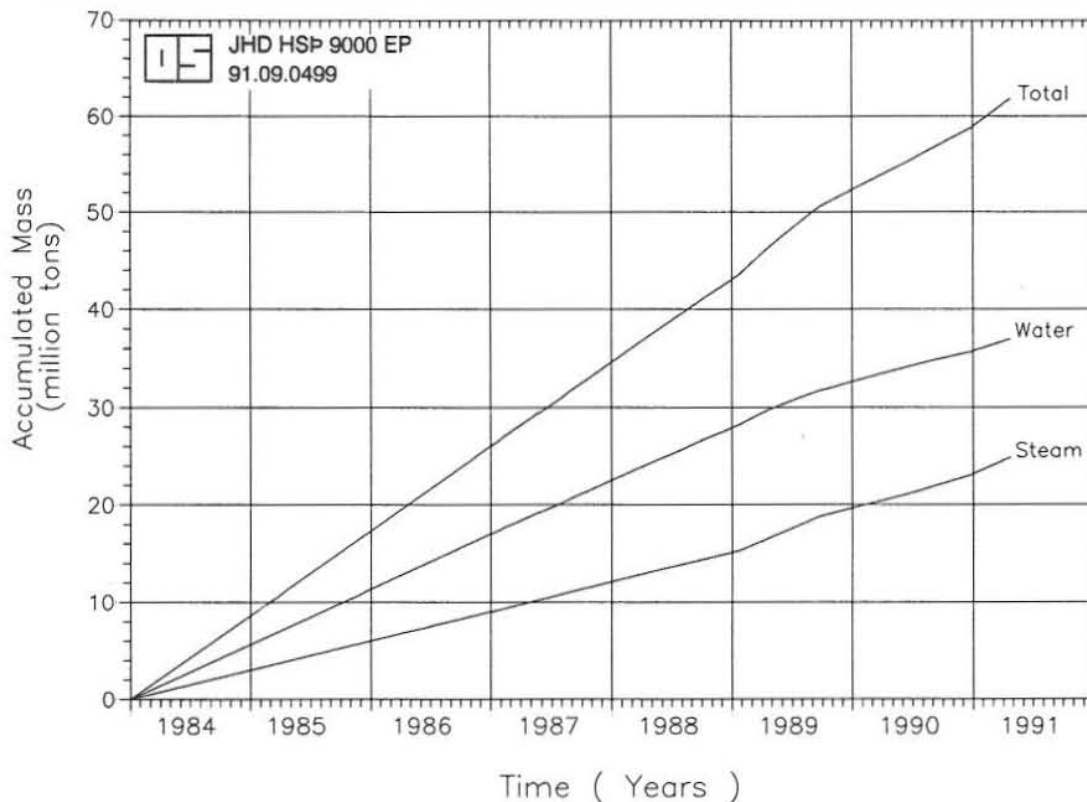


FIGURE 23: Accumulated total, separated water and separated steam production from the Momotombo geothermal field

#### 4.2 Pressure drawdown and permeability

Figure 24 shows the pressure history of the nonproductive well MT-8 at 300 m b.s.l.. Initial pressure in the well, after drilling, is not known, but can be estimated from Girelli's report (1977) as 63 bars-g. The figure shows that more than 17 bars pressure drawdown has occurred since 1976. The closest productive well to MT-8 is MT-31, which produced initially for seven months in 1989 and then again in 1991. The drawdown in MT-8 cannot be explained by the production from MT-31, since no pressure recovery took place after MT-31 was closed in 1989. The drawdown is, therefore, mostly due to production from wells farther away than MT-31. This indicates good horizontal permeability between MT-8 and other productive wells in Momotombo and a large area of drawdown.

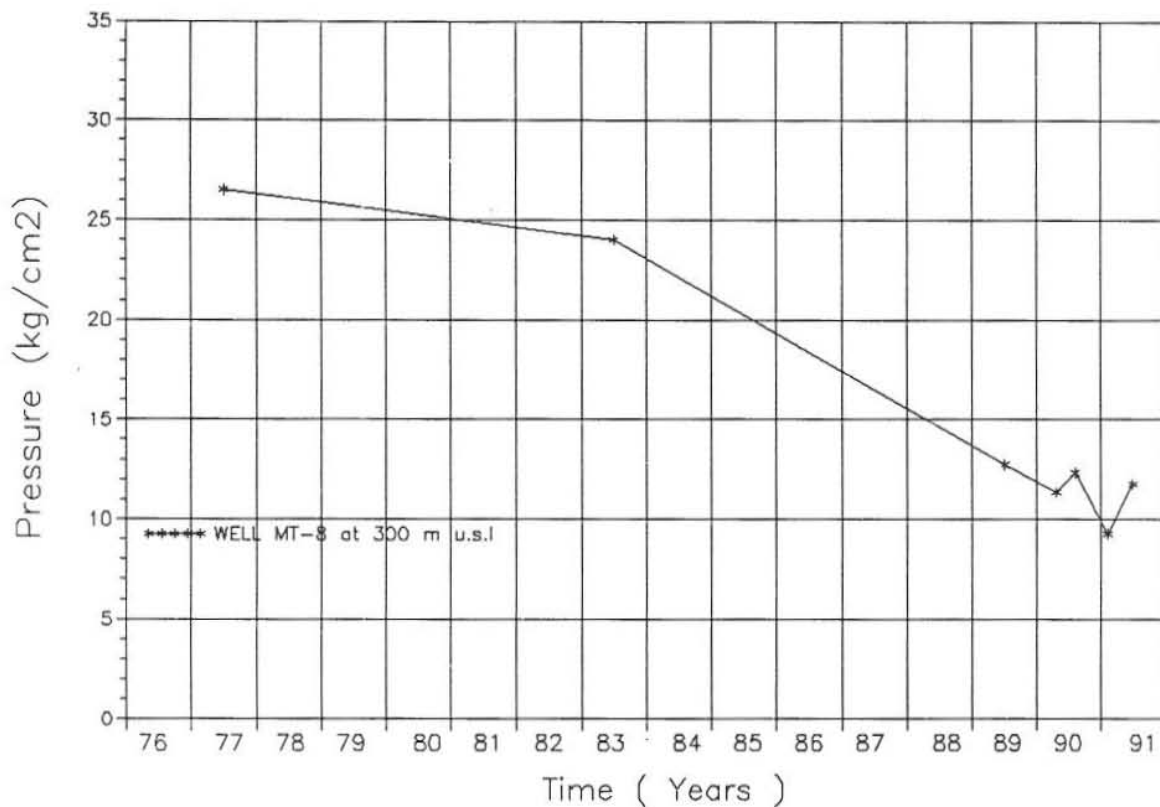


FIGURE 24: Pressure history of well MT-8 at 300 m b.s.l.

Figure 25 shows the pressure history of well MT-13 at 450 and 650 m b.s.l. No production has taken place from the well, at least since 1986. Figure 25 shows that a drawdown rate of 2.5 bars/year took place between 1982 and 1989, when only Unit 1 wells were producing. The pressure in the well, on the other hand, remains stable after 1989. This stability indicates that extensive boiling occurs in the reservoir. Fluid is no longer taken from storage by liquid water expansion and compression of pores, but by steam expansion in the pores as pressure in the reservoir declines to the saturation pressure of the formation.

Figure 26 shows enthalpies of wells MT-12 and MT-20 during the discharge of well MT-9 from June to November, 1988. Substantial enthalpy interference is seen, and is due to decreased reservoir pressure and increased steam saturation in the reservoir between these wells. The data indicates that permeability is high between the wells and that two-phase conditions were established in the productive reservoir at this time.

#### 4.3 Enthalpy changes in initially liquid-saturated reservoirs

The most striking conclusion from the analysis of the production data, is the **enthalpy increase** of the produced fluid in 1989. This phenomena may have a combination of two explanations:

- i) Boiling in the reservoir as the pressure falls under the saturation pressure of the formation.
- ii) The mobile steam enters a well more freely than the liquid water when a two-phase zone is formed around the well.

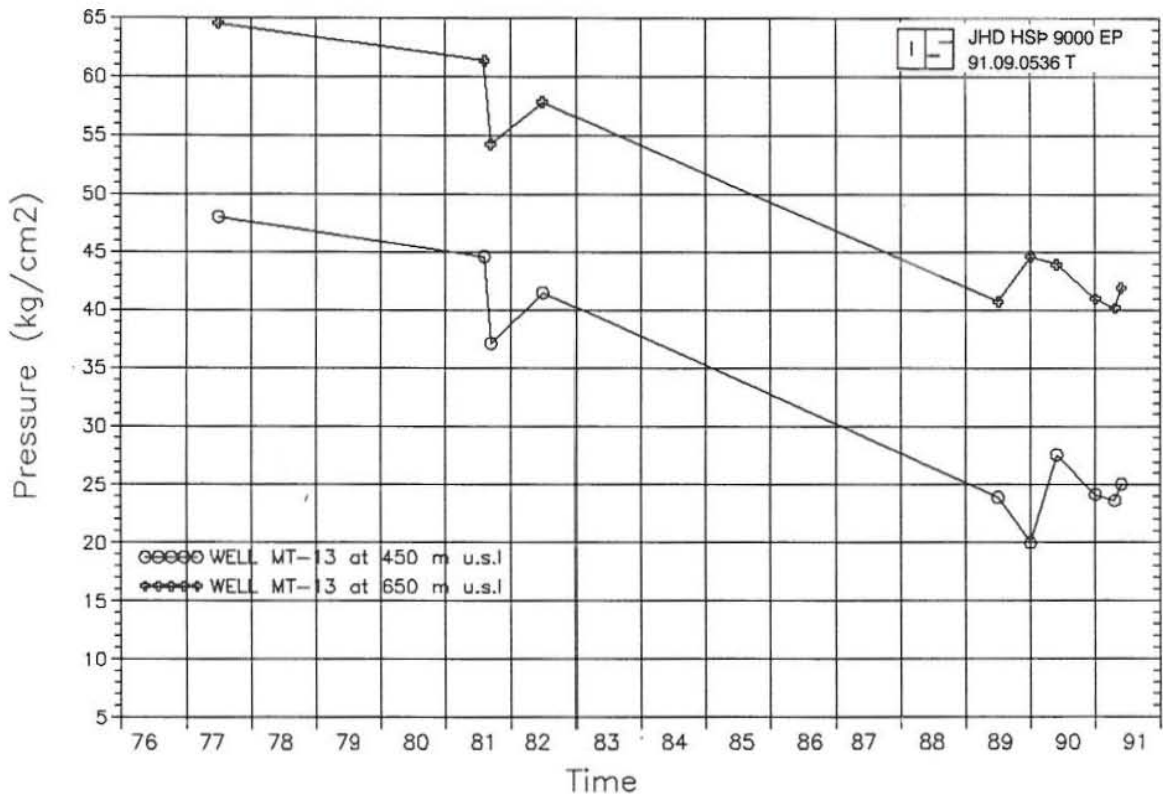


FIGURE 25: Pressure history of well MT-13 at 450 and 650 m b.s.l.

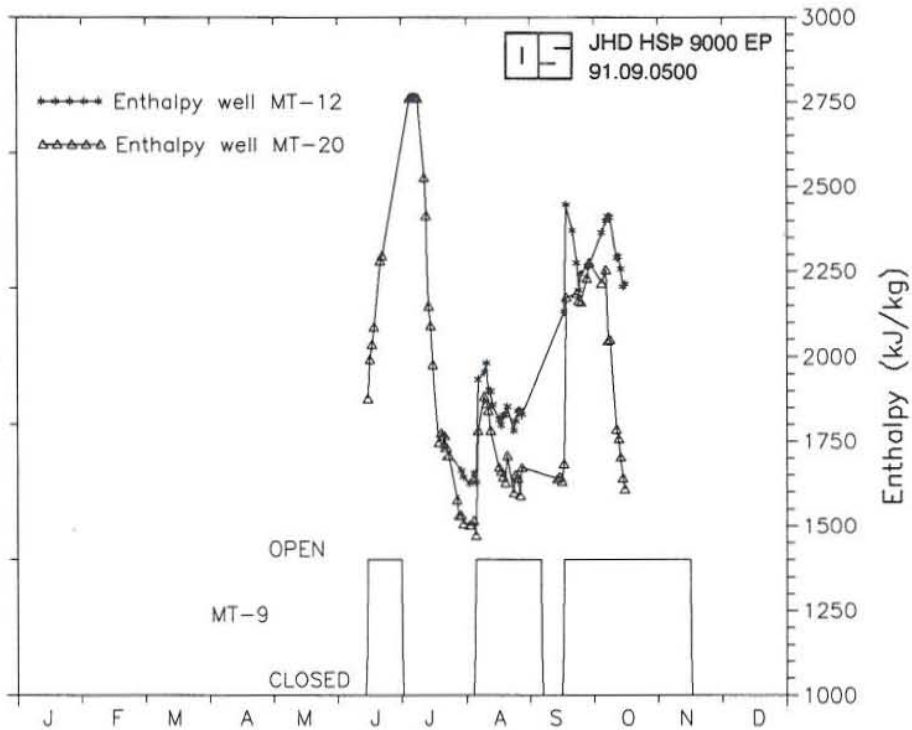


FIGURE 26: Enthalpy changes in wells MT-12 and MT-20 during discharge of well MT-9



### 4.3.1 Extensive boiling

The pressure drawdown, induced by production from a well, will eventually create a boiling in a high temperature, liquid-dominated reservoir. The fluid temperature, at the first stage of boiling, is the same as the formation temperature, but as the fluid pressure declines so will the fluid temperature. The formation temperature, on the other hand, is near-stable. This leads to thermal gradient and a heat flow from the formation to the pore fluid. The energy gained by the fluid increases its enthalpy and, consequently, the production enthalpy of the well. The reservoir pressure, on the other hand, will stabilize as is seen in Figure 25.

### 4.3.2 Mobility effects

The pressure drawdown in a production well may form a small, two-phase zone in and around a feedzone of the well. The state of the flow in this zone will vary substantially from what occurs in the single-phase liquid reservoir. The steam occupies much greater volume due to its low density, and the steam viscosity is much lower than that of liquid water, making the steam more mobile. This leads to a higher mass fraction of steam in the flow into the well and, hence, higher enthalpy of the well.

A two-phase flow in a reservoir can be defined by a Darcy equation of the form (Bodvarsson and Witherspoon, 1989):

$$q_l + q_s = -kA \left[ \frac{k_{rl}}{\mu_l} \rho_l \nabla P + \frac{k_{rs}}{\mu_s} \rho_s \nabla P \right] \quad (24)$$

where  $q$  is the mass flowrate across an area  $A$  in the reservoir,  $k$  is the intrinsic permeability of the cross-section  $A$ ,  $\rho$  is density,  $\nabla P$  is the pressure gradient driving the flow and  $\mu$  is dynamic viscosity. The subscripts  $l$  and  $s$  stand for liquid and steam, respectively, and  $k_{rl}$  and  $k_{rs}$  are the relative permeabilities of liquid and steam. The most simplified relationship for the relative permeabilities is given by the so-called X-Curves, where

$$\begin{aligned} k_{rs} &= S_r \\ k_{rl} &= 1 - S_r \end{aligned} \quad (25)$$

Here,  $S_r$  stands for the volumetric saturation of steam in the reservoir.

Combining Equations 24 and 25 gives, for the ratio of steam flow to the ratio of water flow in the reservoir,

$$\frac{q_s}{q_l} = \frac{S_r}{1 - S_r} \frac{\mu_l \rho_s}{\mu_s \rho_l} \quad (26)$$

Figure 27 shows the ratio  $\mu_l/\mu_s$  and  $\rho_s/\rho_l$  for pure water on the saturation line. Taking 230°C as an average temperature for the shallow Momotombo reservoir gives  $\mu_l/\mu_s = 6.8$  and  $\rho_s/\rho_l = 0.017$ . This simplifies Equation 26 to

$$\frac{q_s}{q_l} = 0.12 \frac{S_r}{1 - S_r} \quad (27)$$

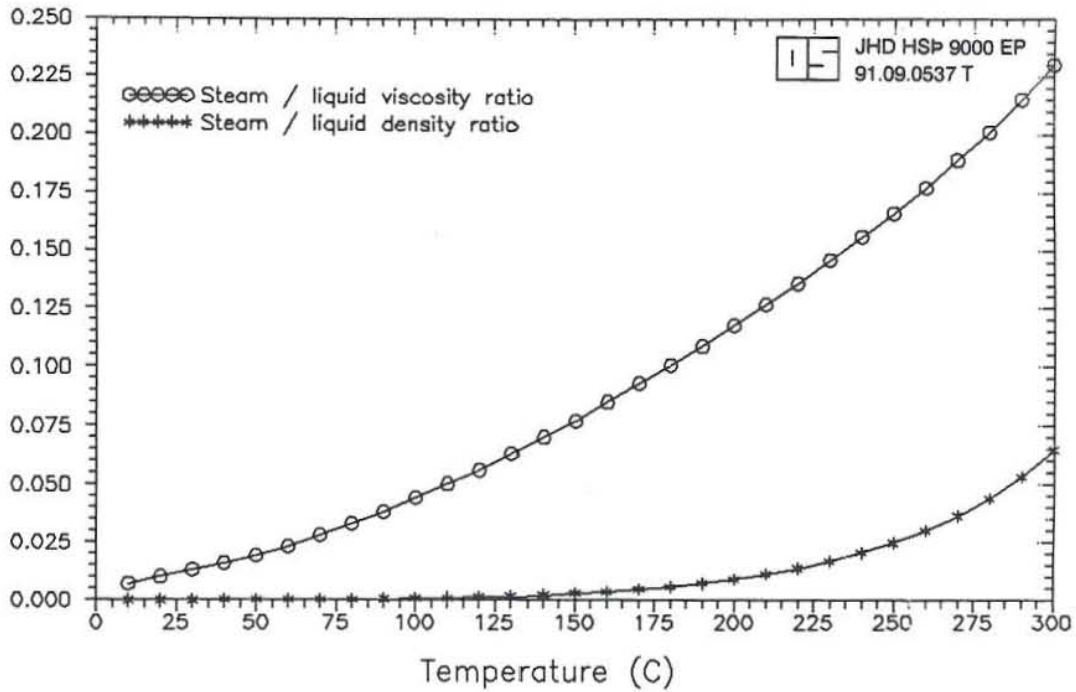


FIGURE 27: Density and dynamic viscosity ratios as a function of the saturation temperature

Figure 28 shows the ratio of the flowrates as a function of the steam saturation  $S_r$  compiled by Equation 27. The figure shows that steam flowrate becomes substantial when the reservoir saturation exceeds 0.5. It is of interest to plot the enthalpy of the flowing fluid in the reservoir as a function of the in situ reservoir mass fraction of steam,  $X_r$ . The steam saturation  $S_r$  is related to  $X_r$  by

$$S_r = \frac{X_r \rho_l}{\rho_s + X_r (\rho_l - \rho_s)} \quad (28)$$

The flowing enthalpy in the reservoir  $h_r$  can be related to the flowrate ratio in (27) by the expression

$$h_r = \frac{\frac{q_s}{q_l} h_s + h_l}{\frac{q_s}{q_l} + 1} \quad (29)$$

Figure 29 shows the flowing enthalpy as a function of the mass fraction of steam in the reservoir as defined by Equations 27-29.

It is of interest to correlate the flowing enthalpy of a well with the mass fraction of steam in the reservoir. This is possible in reservoirs where the intrinsic permeability is high and, hence, with minor pressure gradients  $\Delta P$  between the well and the reservoir (Equation 24). Minor pressure gradient means that the temperature of the flowing fluid and of the formation is nearly equal and, hence, there is no enthalpy increase due to heat flow from formation to the fluid. As an example,

if the average 1800 kJ/kg enthalpy in 1991 (Figure 22) is only due to mobility effects in a 230°C reservoir, then the mass fraction of steam in the reservoir is on the order of 10% and the volumetric fraction of steam is near 87%.

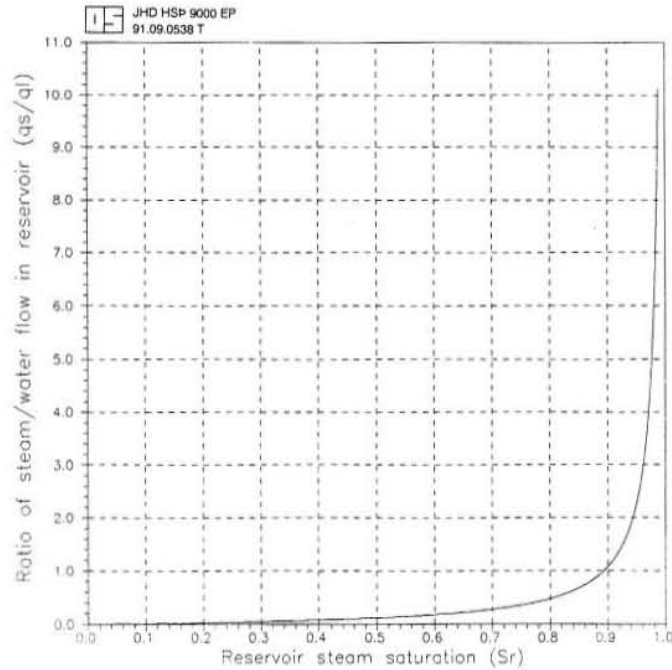


**FIGURE 28:** Ratio of steam and liquid water flowrates as a function of reservoir steam saturation ( $S_r$ ). The reservoir is initially liquid saturated and its temperature is 230°C for all saturation

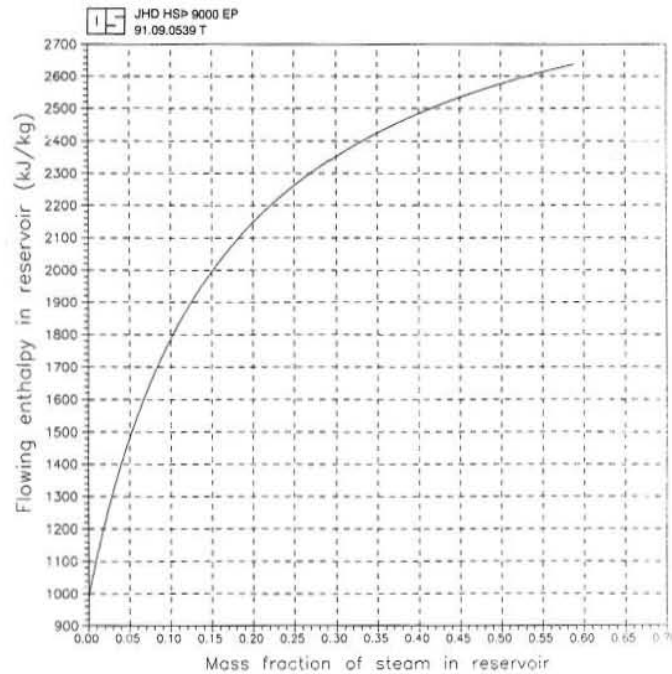


**FIGURE 29:** Relationship between flowing enthalpy and mass fraction of steam in a reservoir of 230°C, which is initially liquid saturated

#### 4.4 Interpretation of enthalpy changes in the Momotombo reservoir

Table 4 shows estimated depths to major feedzones of Momotombo wells, their initial and present enthalpies and the approximated time of an enthalpy increase. The data is taken from Manuel González's report (1990). The table shows that the wellhead enthalpy increases with decreasing depth to feedzones. Figure 30 illustrates this behaviour. The figure shows the wellhead enthalpy in 1991 as a function of depth to feedzones in m b.s.l. Three zones of reservoirs conditions are marked on the figure:

- 1) Zone of dry steam conditions in the reservoir.
- 2) Two-phase flow in feedzones with mobility increase in enthalpies and boiling in some parts of the reservoir.
- 3) Single-phase liquid conditions.

Wells MT-12, MT-20, and MT-31 produce dry steam only. Their feedzones are at depths shallower than 300 m b.s.l. These wells are most likely producing from a dry steam reservoir, which resides down to approximately 250 m b.s.l.

TABLE 4: Estimated depths to major feedzones of Momotombo production wells and dates of enthalpy increase of the produced fluid

Well number	Depth to feedzones (m b.s.l)	Initial feedzone temperature	Initial enthalpy (kJ/kg)	Present enthalpy (kJ/kg)	Date of enthalpy increase
MT-2	320	220°C	940	2550	Before June 1990
MT-9	200 - 600		1050		Liquid saturated in 1988
MT-12	230 - 300	220°C	940	2770	Gradual increase 1987 - 1989
MT-17	230 - 260	225°C	970	1800	Before January 1991
MT-20	230	225°C	970	2770	Before 1987
MT-22	280	210°C	900	1350	
MT-23	430 - 580	255°C	1110	1200	In 1990
MT-26	400 - 500	250°C	1090	1075	No changes
MT-27	213 - 313	240°C	1040	2000	March 1989
MT-31	149 - 299	240°C	1040	2770	In 1989
MT-35	1231	280°C	1240	1750	Before January 1991

Wells MT-2, MT-17, MT-22 and MT-27 produce steam/water mixtures at different enthalpies. The enthalpy increase is most likely due to boiling in the reservoir and in the feedzones. The interval of a two-phase boiling zone in the reservoir is estimated at 250-320 m b.s.l. The mass fraction of steam in the reservoir  $X_r$  can be estimated for the vicinity of well MT-27. The well produced around 80 kg/s when the reservoir was in single-phase liquid conditions. This high flowrate indicates minor drawdown between the well and the reservoir. Furthermore, this means that the mobility analysis in Chapter 4.3.2 applies for the fluid produced from the well. For the 2000 kJ/kg enthalpy of MT-27,  $X_r$  is around 15% and  $S_r$  around 92% (see Figure 29).

At depths greater than 320 m b.s.l. only single-phase liquid condition resides in the reservoir and in the feedzones. An exception is well MT-35 which produces from the deep reservoir. This well is discharging at a great pressure drawdown, inducing localized boiling in its feedzone at 1200 m depth and in the reservoir close to the well.

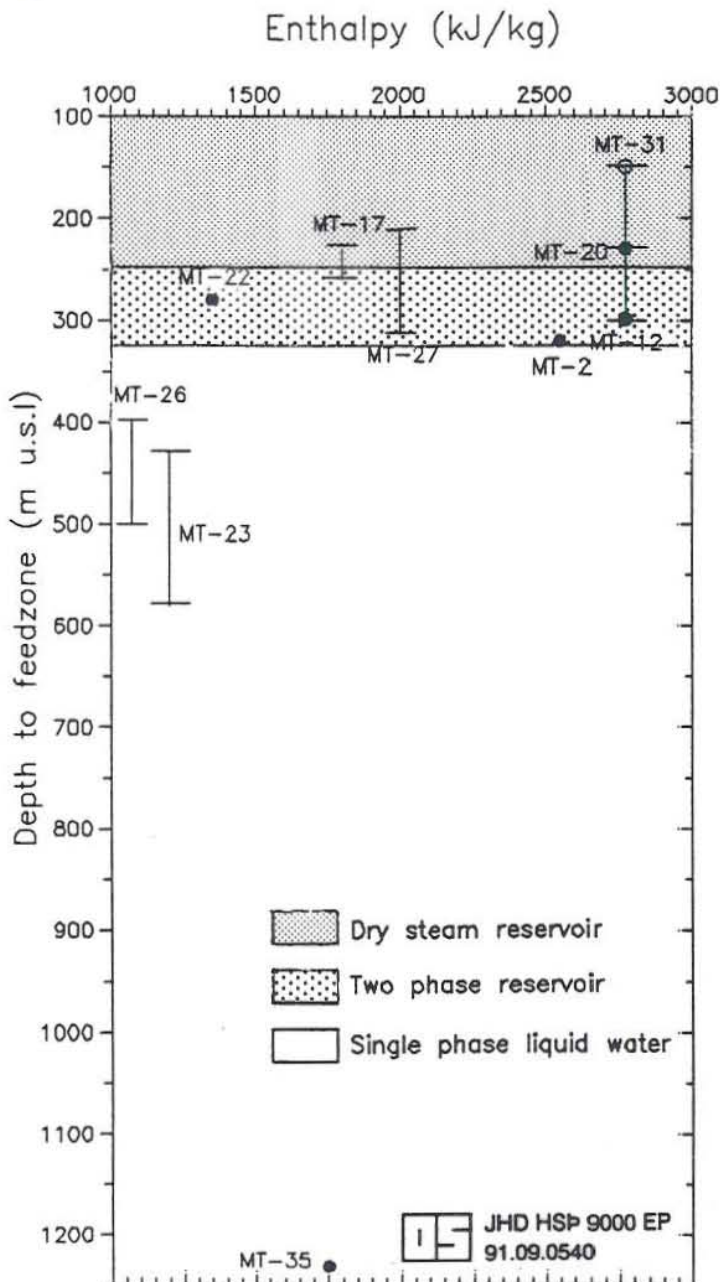


FIGURE 30: Wellhead enthalpy in 1991 as a function of depth to feedzones and estimated state of the shallow reservoir

## 5. VOLUMETRIC MASS CALCULATIONS

### 5.1 Initial mass in storage

It is interesting to compare the cumulative mass production, shown in Figure 23, with the initial fluid mass in storage in the Momotombo reservoir. Such an analysis requires information on the reservoir volume, effective porosity and density of the fluid in the pores.

As most of the produced fluid is taken from shallow reservoir wells, the calculations will concentrate on the shallow reservoir volume. Figure 31 shows the estimated initial temperature distribution in Momotombo at 300 m b.s.l. (González Solórzano, 1990). This depth is representative for the shallow reservoir. The areal extent of the reservoir is estimated as 1 km<sup>2</sup> from the 210°C isotherm in Figure 31, which is taken to be the outer limit of the reservoir. The thickness is assumed to be 300 m, also from the initial temperature distribution (González Solórzano, 1990). This gives a total volume of 3x10<sup>8</sup> m<sup>3</sup>.

The shallow reservoir was initially liquid-saturated (Girelli et al., 1977; González Solórzano, 1990). The water density in the pores,  $\rho_r$ , was then around 840 kg/m<sup>3</sup>, assuming an average temperature of 230 °C for the reservoir.

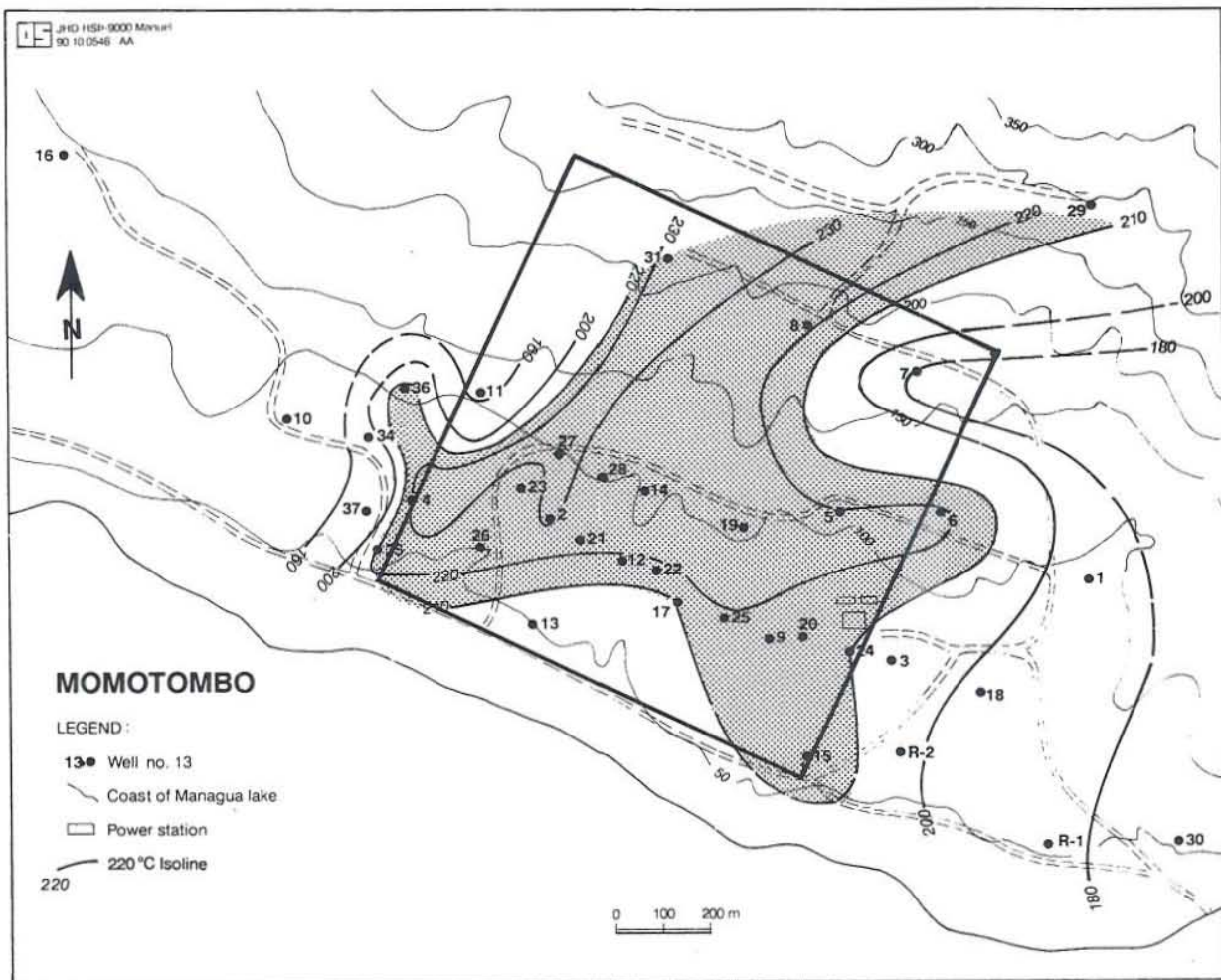


FIGURE 31: Initial temperature distribution at 300 m b.s.l. (González Solórzano, 1990). The area of the rectangular box is 1 km<sup>2</sup> and the area within the 210°C isoline is shaded

The fluid mass in storage,  $m_{st}$ , in the shallow Momotombo reservoir is then given by

$$m_{st} = \phi \rho_r V_{rock} = \phi \times 827 \times 3 \times 10^8 \quad (30)$$

where  $\phi$  is the effective reservoir porosity.

Table 5 shows the percentage of the initial fluid mass withdrawn, for different porosities. The mass produced is taken from Figure 23 as  $6.2 \times 10^{10}$  kg minus  $0.2 \times 10^{10}$  kg which is the cumulative mass produced from deep reservoir wells.

The porosity of the shallow reservoir is not known. The reservoir rock is sedimentary (Ferrey, 1977) which implies high porosity, probably on the order of 20 % (Bjornsson and Bodvarsson, 1990). This means that a substantial fraction of the initial fluid in storage in the shallow reservoir has already been produced. This also means that basically, the present production depends on the natural recharge to the system and on reinjection.

TABLE 5: Percentage of initial fluid in storage withdrawn from the Momotombo reservoir

Porosity ( $\phi$ )	Initial mass in storage (kg)	Mass produced 1983 - 1991 (kg)	Percentage withdrawn (%)
0.05	$1.2 \times 10^{10}$	$6.0 \times 10^{10}$	483
0.10	$2.5 \times 10^{10}$	$6.0 \times 10^{10}$	241
0.15	$3.7 \times 10^{10}$	$6.0 \times 10^{10}$	161
0.20	$5.0 \times 10^{10}$	$6.0 \times 10^{10}$	121
0.25	$6.2 \times 10^{10}$	$6.0 \times 10^{10}$	97
0.30	$7.4 \times 10^{10}$	$6.0 \times 10^{10}$	80

## 5.2 Natural recharge

Figure 30 shows that around half of the shallow reservoir is still liquid-saturated. Table 5 therefore indicates that natural recharge to the shallow reservoir is substantial, assuming a reservoir porosity of 20%. The rate of the recharge can be estimated by the following volumetric calculations.

The analysis of enthalpy data show that three conditions of state occur in the shallow reservoir, a dry steam zone at 150-250 m b.s.l., a two-phase zone of high volumetric steam saturation at 250-320 m b.s.l., and a liquid-saturated zone at 320-450 m b.s.l. (Figure 30). The residual mass of liquid in this volume,  $m_{res}$ , is then

$$m_{res} = V_1 \rho_s + V_2 \rho_s S_r + V_2 \rho_l (1 - S_r) + V_3 \rho_l \quad (31)$$

where  $V_{1,2,3}$  are the pore volumes of the three zones,  $\rho_l$  and  $\rho_s$  are the saturation densities of liquid and steam at 230°C, and  $S_r$  is the volume fraction of steam in the two-phase zone (Figure 32). Taking  $\phi = 20\%$  and  $S_r = 80\%$ , gives for Equation 31 that  $m_{res} = 2.4 \times 10^{10}$  kg.

The natural recharge rate is then defined by the following mass conservation

$$m_c + m_{res} = m_{st} + m_{nat} + m_{reinj} \quad (32)$$

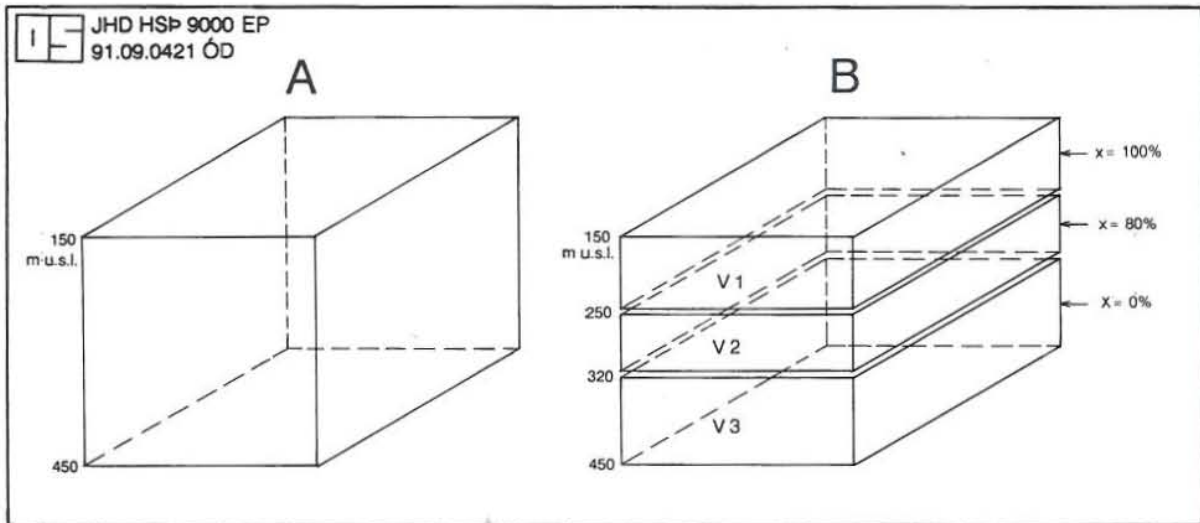


FIGURE 32: Volumes of water and steam in the shallow reservoir, A) prior to production; B) in 1991

where  $m_c$  is the cumulative mass produced ( $6 \times 10^{10}$  kg),  $m_{nat}$  is the natural recharge to the volume under consideration and  $m_{reinj}$  is the reinjected mass to the system.

The reinjected water mass into the reservoir is, for the eight years of production, around  $1.4 \times 10^{10}$  kg (Arcia Róger, personal communication, 1991). The initial mass in storage is taken from Table 5 as  $5 \times 10^{10}$  kg ( $\phi = 20\%$ ). Inserting terms and solving Equation 32 gives that  $m_{nat} = 2 \times 10^{10}$  kg.

This high fraction of natural recharge indicates that, either the volume of the shallow reservoir is underestimated, or that the pressure drawdown in the shallow reservoir draws a substantial amount of fluid mass from deeper parts of the system. An answer to this question is beyond the scope of this report.

### 5.3 Future performance of the shallow reservoir

The simple analysis in Chapters 5.1 and 5.2 enables one to roughly predict the future response of the shallow reservoir to production. The present production has withdrawn around 50% of the initial fluid mass in the shallow reservoir. It is of interest to predict how long a time it takes to fully deplete all this mass. Figure 33 shows hypothetical cumulative production from the Momotombo field, assuming three different production cases. First of all, the present slope of total production is extended to the year 2000 (total production of 300 kg/s, Figure 22), secondly 80% of the separated water is reinjected (80% of 125 kg/s) and finally the case where only steam is produced (175 kg/s) is taken into consideration. If the shallow reservoir accounts for 40% of the future mass production, then the present  $2.4 \times 10^{10}$  kg of fluid in storage will be depleted when another  $6 \times 10^{10}$  kg have been produced. This will happen, according to Figure 33, in the time period 1997-2001. The consequence of the depletion of the shallow reservoir will be a dramatic reduction in flowrates from the present wells.



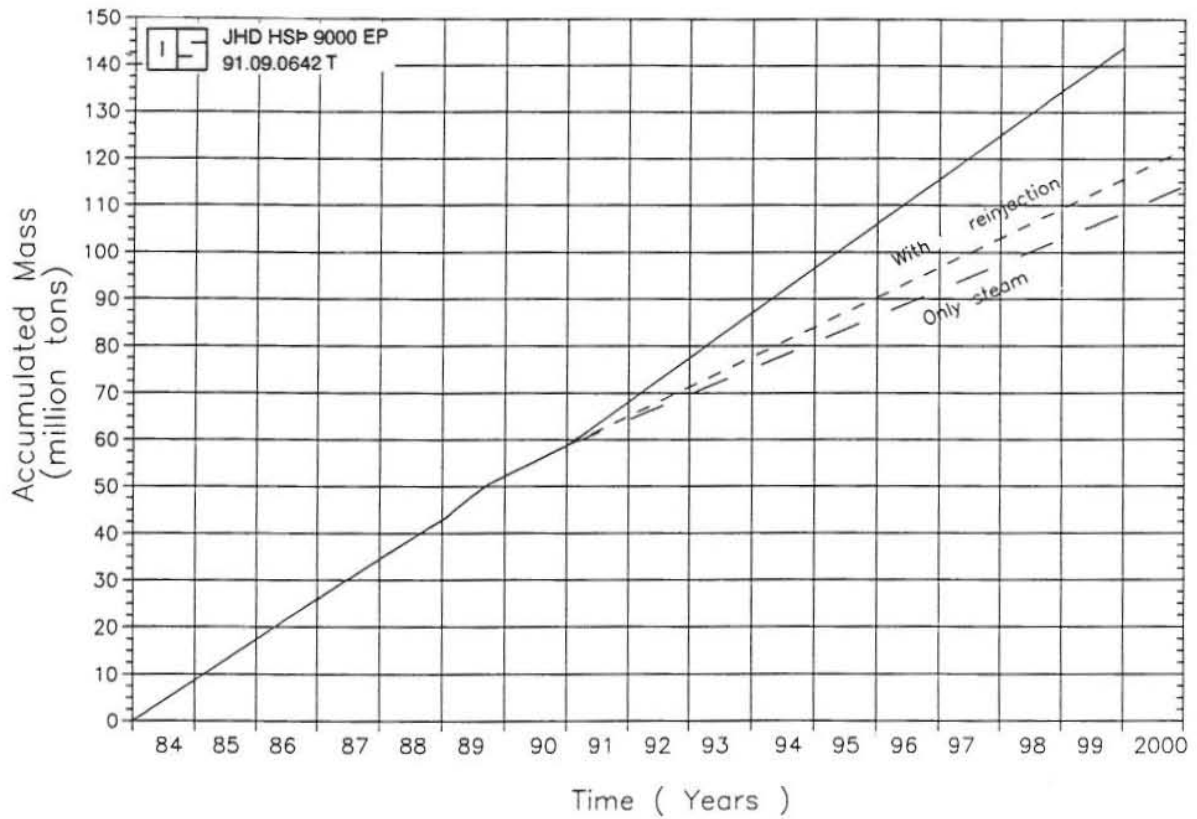


**FIGURE 33:** Predicted cumulative production from Momotombo. The fluid mass in the shallow reservoir may be depleted after the production of 120 million tons

## 6. CONCLUSIONS AND RECOMMENDATIONS

The main conclusions of this report are the following:

1. The equations, which have been used to calculate total flowrates and enthalpies from Momotombo wells, have been verified.
2. Substantial changes occurred in wellhead flowrates and enthalpies when total production was doubled in 1989. Enthalpies have, in general, increased and separated water flowrates decreased, whereas steam flowrates are nearly constant.
3. Decline rates of wellhead pressures and total flowrates have increased in the year 1991, when Unit 2 again came on-line.
4. The shallow reservoir seems to be of high permeability which is reflected in substantial enthalpy interference between wells and a large area of drawdown.
5. More than 20 bars pressure drawdown has occurred in the shallow reservoir. The drawdown area extends north to well MT-8.
6. The great pressure drawdown has induced extensive boiling in the reservoir. Volumetric expansion of liquid water to steam maintains the reservoir pressure at present.
7. Good correlation is observed between flowing enthalpies of wells and depths to major feedzones, where the enthalpy decreases with depth. This is interpreted by a three layer shallow reservoir model. The uppermost layer, at 150-250 m b.s.l., contains only steam; at 250-320 m b.s.l. resides a two-phase layer and beneath 320 m b.s.l., the reservoir is liquid-saturated.
8. A study of mobility effects indicates that the volumetric steam saturation in the two-phase zone is on the order of 80-90%.
9. The shallow reservoir initially had around  $5 \times 10^{10}$  kg of liquid water in storage. The cumulative production, on the other hand, is around  $6 \times 10^{10}$  kg.
10. The natural recharge to the shallow reservoir is on the order of  $2 \times 10^{10}$  kg, when taking into account fluid mass in storage and reinjection.
11. If the contribution of the shallow reservoir to the total flow remains the same in the future, as in the past, only 6-10 years may pass until the reservoir is fully depleted. At that time, flowrates from present wells may have declined drastically.

In summary, the main conclusion of the study is that the present wellfield is too small to generate steam for a 70 MW<sub>e</sub> power station for the next 20-30 years. More drilling into the deep reservoir is necessary in order to maintain steam production rates in the future. A detailed well-by-well reservoir simulation is also essential for optimizing future production from the field. A simulation study might, for example, reduce the risk of overcooling the shallow reservoir by reinjection.

## ACKNOWLEDGEMENTS

I would like to express my gratitude to Mr. Grimur Bjornsson for his excellent supervision, advice and evaluation of the work presented in this report.

Thanks go to Dr. Ingvar Birgir Fridleifsson, director of the UNU Geothermal Training Programme for providing excellent work conditions, to "Uncle" Ludvik S. Georgsson for his excellent attention and guidance throughout the training course, to our teachers, and special thanks go to Josef Holmjarn for his valuable assistance with the computer and all the staff of scientists at ORKUSTOFNUN.

Special thanks go to Eng. Ernesto Martínez Tiffer for his continuous support, Eng. Róger Arcia, Eng. Melba Sú and all the staff at Recursos Geotérmicos (Instituto Nicaragüense de Energía) for providing fundamental information for the study and finally, very special thanks go to my mother for whom I really did my best.

## NOMENCLATURE

$A$	: Cross-section area in the reservoir, $m^2$
$A_d$	: Cross-sectional area of the discharge pipe, $cm^2$
$A_1$	: Cross-sectional area of the upstream section, $m^2$
$A_2$	: Cross-sectional area of the downstream section, $m^2$
$C_d$	: Coefficient of discharge for the thin-plate orifice
$C$	: Discharge coefficient for the V-notch
$D$	: Diameter of pipe at upstream section, $cm$
$d$	: Diameter of thin-plate orifice, $cm$
$F_a$	: Thermal expansion factor
$G$	: Total flow per unit area in a pipe, $kg/cm^2 / s$
$g_c$	: Proportional constant, 9.80652
$g$	: Acceleration of gravity, 9.80652 $m/s^2$
$h_t$	: Total enthalpy from the well, $kJ/kg$
$h_{sa}$	: Enthalpy of steam at atmospheric conditions, $kJ/kg$
$h_{la}$	: Enthalpy of liquid at atmospheric conditions, $kJ/kg$
$h_1$	: Total enthalpy in the upstream section, $kJ/kg$
$h_2$	: Total enthalpy in the downstream section, $kJ/kg$
$h_{ls}$	: Enthalpy of liquid at the separator pressure, $P_s$ , $kJ/kg$
$h$	: Height of a column of flowing fluid producing the flow over a weir, $m$
$h_r$	: Flowing enthalpy in the reservoir, $kJ/kg$
$h_s$	: Flowing enthalpy of steam in the reservoir, $kJ/kg$
$h_l$	: Flowing enthalpy of liquid in the reservoir, $kJ/kg$
$h_{ss}$	: Enthalpy of steam at separator pressure, $P_s$ , $kJ/kg$
$k$	: Intrinsic permeability of the reservoir, $m^2$
$k_{rl}$	: Relative permeability of liquid
$k_{rs}$	: Relative permeability of steam
$L_c$	: Width of approach channel upstream of a weir, $m$
$m_t$	: Total flowrate from the well, $kg/s$
$m_{la}$	: Liquid water flowrate measured in a weir box, $kg/s$
$m_{res}$	: Residual mass of the fluid in the shallow reservoir, $kg$
$m_c$	: Cumulative mass produced, $kg$
$m_{nat}$	: Natural recharged mass to the shallow reservoir, $kg$
$m_{reinj}$	: Reinjecting mass to the shallow reservoir, $kg$
$m_{sa}$	: Steam flowrate at atmospheric conditions, $kg/s$
$m$	: Flowrate through a thin-plate orifice, $kg/s$
$m_{ls}$	: Water flowrate after the separator, $kg/s$
$m_{ss}$	: Steam flowrate after the separator, $kg/s$
$m_{st}$	: Fluid mass in storage, $kg$
$P_{lip}$	: Lip pressure, $MPa$
$P_1$	: Upstream pressure, $bar-a$
$P_2$	: Downstream pressure, $bar-a$
$P_s$	: Separator pressure, $bar-a$
$P$	: Elevation of triangular-notch weir above bottom of approach channel, $m$
$q_w$	: Heat transferred to or from the fluid
$q$	: Total theoretical volumetric flowrate, $m^3/s$
$q_l$	: Liquid mass flowrate across an area $A$ of the reservoir, $kg/s$
$q_s$	: Steam mass flowrate across an area $A$ of the reservoir, $kg/s$
$r$	: Ratio of pressure, $P_2/P_1$
$Re_D$	: Reynolds number based on diameter $D$

- $S_r$  : Volumetric saturation of steam in the reservoir  
 $u_{k1}$  : Kinetic energy of the flow in the upstream section, kJ/kg  
 $u_{k2}$  : Kinetic energy of the flow in the downstream section, kJ/kg  
 $u_{i1}$  : Internal energy of the fluid in the upstream section, kJ/kg  
 $u_{i2}$  : Internal energy of the fluid in the downstream section, kJ/kg  
 $V_1$  : Pore volume in the steam zone of the reservoir, m<sup>3</sup>  
 $V_2$  : Pore volume in the two-phase zone of the reservoir, m<sup>3</sup>  
 $V_3$  : Pore volume in the liquid-saturated zone, m<sup>3</sup>  
 $V_{rock}$  : Volume of the reservoir, m<sup>3</sup>  
 $V_u$  : Average velocity of the fluid in the upstream section, m/s  
 $V_d$  : Average velocity of the fluid in the downstream section, m/s  
 $V_s$  : Theoretical velocity of a stream filament in the V-notch, m/s  
 $x_a$  : Mass fraction of steam at atmospheric conditions  
 $X_r$  : Reservoir mass fraction of steam  
 $Y$  : Expansion factor of steam  
 $y$  : Distance between a stream filament with velocity  $V_s$  and the surface of the fluid flow through a V-notch, m  
 $z_1$  : Elevation of a datum in the upstream section, m  
 $z_2$  : Elevation of a datum in the downstream section, m

## Greek letters:

- $\alpha$  : Flow coefficient  
 $\beta$  : Ratio of diameters,  $d/D$   
 $\gamma$  : Ratio of specific heats of an ideal gas,  $C_p/C_v$   
 $\Delta P$  : Differential pressure,  $P_1 - P_2$ , bar-a  
 $\theta$  : Bottom angle of a triangular-notch weir, degree  
 $\mu_l$  : Dynamic viscosity of liquid in the reservoir, kg/m/s  
 $\mu_s$  : Dynamic viscosity of steam in the reservoir, kg/m/s  
 $\pi$  : Constant, 3.14159  
 $\rho$  : Fluid density, kg/m<sup>3</sup>  
 $\rho_1$  : Density of the fluid in the upstream section, kg/m<sup>3</sup>  
 $\rho_2$  : Density of the fluid in the downstream section, kg/m<sup>3</sup>  
 $\rho_r$  : Water density in the pores, kg/m<sup>3</sup>  
 $\rho_l$  : Liquid density, kg/m<sup>3</sup>  
 $\rho_s$  : Steam density, kg/m<sup>3</sup>  
 $v_1$  : Specific volume of the fluid in the upstream section, m<sup>3</sup>/kg  
 $v_2$  : Specific volume of the fluid in the downstream section, m<sup>3</sup>/kg  
 $\phi$  : Effective reservoir porosity, ratio

## REFERENCES

- ASME, 1971: Fluid Meters. Their theory and application. The American Society of Mechanical Engineers, New York, 273 pp.
- Bjarnason, J.O., 1985: The fortran library STEAM. Orkustofnun, Reykjavik, report OS-85069/JHD-09 (in Icelandic), 129 pp.
- Bjornsson, G., and Bodvarsson, G., 1990: A survey of geothermal reservoir properties. *Geothermics*, vol. 19-1, 17-27.
- Bodvarsson, G.S., and Witherspoon, P., 1989: Geothermal reservoir engineering - part 1. *Geothermal Sciences and Technology*, vol. 2-1, 1-68.
- Ferrey, C., 1977: Geology of the Momotombo geothermal field. Momotombo Geothermal Project (in Spanish), Managua, Nicaragua.
- Fox, R., and McDonald, A., 1985: Introduction to fluid mechanics. School of Mechanical Engineering, Purdue University, 741 pp.
- Girelli, M., Saltuklaroglu, M., and Vega, R., 1977: A case history of Momotombo geothermal field. *Publicación del Instituto Italo-Latino Americano*, Roma, 251-271.
- González Solórzano M., 1990: Initial temperature distribution in the Momotombo geothermal field, Nicaragua. UNU G.T.P., Iceland, report 6, 43 pp.
- Grant, A., Donaldsson, I., and Bixley, P., 1982: Geothermal reservoir engineering. Academic Press, New York, 368 pp.
- INE, 1989: The Patricio Argüello Ryan geothermal power plant (in Spanish). Instituto Nicaragüense de Energía, Managua, Nicaragua.
- James, R., 1970: Factors controlling borehole performance. UN symposium on the development and utilization of geothermal resources, Pisa, Proceedings - *Geothermics*, Spec. iss. 2, 2, 1502-1515.
- Kasap, I., 1986: Progress report No.1, Results of Mr. Ibrahim Kasap's activities. Instituto Nicaragüense de Energía, internal report, 16 pp.
- Martínez Tiffer, E., Arcia, R., and Sabatino, G., 1988: Geothermal development in Nicaragua. *Geothermics*, 17, no. 2/3, 333-354.
- White, F., 1979: Fluid Mechanics. McGraw-Hill, New York, 307 pp.



**APPENDIX I:**

**A listing of the programs LIP, CUM, MOM, and KASAP**



## Program LIP.F

```

c*****
c
c          PROGRAM LIP
c
c This program calculates flow rates from geothermal wells according
c to the method of Russel James. The input parameters are taken after
c a silencer (V-notch type weir box) and the lip pressure at the end
c of a horizontal discharge pipe.
c
c*****
c
c      program lip
c      implicit none
c      real alp,df,dh,f,ht,h_n
c      real b,dd,ddd,h
c      real kkk,ml,ml1,ml2,mt,pl,x
c      integer ians,nu_it,iq
c
c-----
c Input parameters for geometry of separator and outlet devices
c Pipe diameter changed to cm
c-----
c
c 10  write (6, '(/,10x, ' ***** RUSSEL JAMES EQUATIONS *****', /)')
c     write (6, '( ' Pipe diameter (cm) ..... : ', $)')
c     read (5, *) dd
c
c-----
c Input parameters for the flow itself. Pressure changed to MPa-a
c and height to meters.
c-----
c
c 20  write (6, '( ' The lip pressure (bar-g)..... : ', $)')
c     read (5, *) pl
c     pl = ( pl + 1.013 ) * 0.1
c     write (6, '( ' Water height in the weir (cm) ..... : ', $)')
c     read (5, *) h
c     h = h/100. + 0.00085
c
c-----
c Water flow calculations. The equation is from the book:
c FLUID METERS. Their theory and application. Sixth Edition, 1971.
c The American Society of Mechanical Engineers. Equation I-8-15
c (p 117) is used, assuming C' to be a constant of 0.59 (fig. I-8-9)
c and the V-notch angle, alpha, to be 90 deg.
c-----
c
c     if ( h .gt. 0 ) then
c         ml2 = 1.39*958.*((h+0.00085)**2.5)
c     else
c         ml2 = 0.
c     endif

```

```

c-----
c Iterated for the enthalpy by using equation ?? in final report.
c The iteration scheme used is the one of Newton.
c-----
c
c
c     ht = 1500.
c     nu_it = 0
c 30  f = ml2 - (3.14159*dd*dd*(pl**0.96)*1680.)/(ht**1.102)*
c     1 (2676-ht)/(2676.-419.)
c     dh = ht*1.0001
c     df = ml2 - (3.14159*dd*dd*(pl**0.96)*1680.)/(dh**1.102)*
c     1 (2676-dh)/(2676.-419.)
c     h_n = ht - (f*(ht*0.0001))/(df-f)
c     nu_it = nu_it+1
c     if ( nu_it .gt. 20 ) then
c         write (6, *) ' No solution for this data'
c         ht = 0.
c         mt = 0.
c         goto 40
c     endif
c     write (6,110) nu_it,ht,h_n,f
c 110 format ( ' Nu it',i5, ' Old enth',f8.1, ' New enth',f8.1, ' f',f10.6)
c     ht = h_n
c     if ( abs(f) .gt. 0.0001 ) goto 30
c     x = (ht-419.)/(2676.-419.)
c     mt = ml2 / (1.-x)
c
c-----
c Writing results to the screen
c-----
c
c 40  continue
c     pl = pl*10.-1.013
c     h = (h-0.00085)*100.
c     write (6,100) dd,pl,h,ml2,mt-ml2,mt,ht
c 100 format ( /,10x, ' ***** RESULTS OF CALCULATIONS *****', //,10x,
c 4 ' Pipe diameter (cm)',t50,f10.2,/10x,
c 4 ' Lip pressure (bar-g)',t50,f10.2,/10x,
c 5 ' Water height in veir (cm)',t50,f10.3,/10x,
c 6 ' Water flowrate (kg/s)',t50,f10.2,/10x,
c 7 ' Steam flowrate (kg/s)',t50,f10.2,/10x,
c 8 ' Total flowrate (kg/s)',t50,f10.2,/10x,
c 9 ' Total enthalpy (kJ/kg)',t50,f10.1)
c     write (6,200)
c 200 format ( /,70(' '),/5x, ' Next action : ',/,
c 1 10x, ' 1. Another data for same well <ret>',/,
c 2 10x, ' 2. A new well data',/,
c 3 10x, ' 3. Stop',t50, ' : ', $ )
c     read (5, '(q,i5)') iq,ians
c     if ( ians .eq. 1 .or. iq .eq. 0 ) then
c         goto 20
c     elseif ( ians .eq. 2 ) then
c         goto 10
c     endif
c     stop
c     end

```

## Program KASAP.F

```

c*****
c
c          PROGRAM KASAP
c
c This program calculates flow rates of Momotombo wells according to
c equations presented by Ibrahim Kasap (Momotombo internal report).
c The input parameters are taken after a separator, one group is taken
c on the steam pipe outlet and another in a V-notch type weir box.
c The output is written to a file and on the terminal.
c
c          Grimur Bjornsson, sept. 1991
c*****
c
c          program kasap
c          integer da,mm,yy
c          character*50 out
c          real*8 qs,alpha,y,b,d,dd,gamma,pu,pd,ps,p0,delp
c          real*8 qw,kk,h
c          real*8 hs,hl,rho_s,tsat
c          real*8 h_total,x_atm,x_sep,x_wh
c
c -----
c Input parameters for geometry of separator and outlet devices
c -----
c
10  write (6,'(10x, '***** FLOWRATE CALCULATIONS *****',/)' )
5   write (6,'('' Type of input'',t20,' 1. From keybord',/,t20,
1   ' 2. From a file : ','$)')
   read (5,'(i3)') itype
   if ( itype .eq. 2 ) then
   write (6,'('' Name of input file .....: ','$)')
   read (5,'(a)') out
   open ( unit=1,file=out,status='old' )
   write (6,'('' Name of output file .....: ','$)')
   read (5,'(a)') out
   open ( unit=2,file=out,status='unknown' )
   elseif ( itype .eq. 1 ) then
   write (6,'('' Steam pipe diameter (mm) .....: ','$)')
   read (5,*) dd
   write (6,'('' Orifice diameter (mm) .....: ','$)')
   read (5,*) d
c
c -----
c Input parameters for the flow itself
c -----
c
20  write (6,'('' Wellhead pressure (bar-g) .....: ','$)')
   read (5,*) p0
   write (6,'('' Separator pressure (bar-g) .....: ','$)')
   read (5,*) ps
   write (6,'('' Upstream pressure (bar-g) .....: ','$)')
   read (5,*) pu
   write (6,'('' Downstream pressure (bar-g) .....: ','$)')
   read (5,*) pd
   delp = pu-pd
   if ( delp .le. 0 ) then
   write (6,'('' +++ error in pressures +++''))
   goto 20
   endif
   write (6,'('' Water height in the weir (cm) .....: ','$)')
   read (5,*) h
   else
   goto 5
   endif
c
c -----
c Writing results to the screen
c -----
c
   if ( itype .eq. 1 ) then
   call calculate (p0,ps,pu,pd,dd,d,h,qs,qw,h_total,x_atm,x_sep,x_wh)
   write (6,100) p0,ps,pu,pd,dd,d,h,qs,qw
100  format ( /,10x, ' **** RESULTS OF CALCULATIONS ****',//,10x,
1   ' Wellhead pressure (bar-g) = ',f10.3,/10x,
1   ' Separator pressure (bar-g)= ',f10.3,/10x,
1   ' Upstream pressure (bar-g) = ',f10.3,/10x,
2   ' Downstr. pressure (bar-g) = ',f10.3,/10x,
3   ' Pipe diameter (mm) = ',f10.2,/10x,
4   ' Orifice diameter (mm) = ',f10.2,/10x,
5   ' Water height in veir (m) = ',f10.3,//10x,
7   ' Steam sep. flowr. (kg/s) = ',f10.2,/10x,
7   ' Liquid sep. flowr. (kg/s) = ',f10.2 )
150  write (6,150) h_total,qw+qs,x_atm,x_sep,x_wh
   format ( 10x,
1   ' Total enthalpy (kJ/kg) = ',f10.3,/10x,
2   ' Total flowrate (kg/s) = ',f10.2,/10x,
3   ' Steam fraction at 1 bar-a = ',f10.3,/10x,
4   ' Steam fraction at separ. = ',f10.3,/10x,
5   ' Steam fraction at wellh. = ',f10.3 )
   write (6,200)
200  format ( /,70(' '),/,5x, ' Next action : ',/,
1   10x, ' 1. Another data for same well',/,
2   10x, ' 2. A new well data',/,
3   10x, ' 3. Stop',20x, ' : ','$ )
   read (5,*) ians
   if ( ians .eq. 1 ) then
   goto 20
   elseif ( ians .eq. 2 ) then

```

```

        goto 10
    endif
c
-----
c Calculating data from input file
-----
c
    else
    read (1,*)
    read (1,*)
    read (1,*)
    write (2,60)
    write (2,70)
    write (2,'( 50(''-'' )')')
60  format ('dd mm yy Days Po Tot Steam Water Enth Xa Xs')
70  format ('          barg kg/s kg/s kg/s kJ/kg')
    do 300 i=1,1000
    read (1,105,end=999) da,mm,yy,dd,d,p0,ps,pu,pd,h
105  format (i2,1x,i2,1x,i2,2f7.1,2f6.1,2f7.2,f7.1)
    call calculate (p0,ps,pu,pd,dd,d,h,qs,qw,h_total,x_atm,x_sep,x_wh)
    days = (yy-87)*365.25 + (mm-1)*30.4 + da
    write (2,205) da,mm,yy,days,p0,qs+qw,qs,qw,h_total,x_atm,x_sep
205  format (i2,'-',i2,'-',i2,f8.1,f5.1,3f6.1,f6.0,2f5.2)
300  continue
999  continue
    endif
    stop
    end
c
c*****
c          SUBROUTINE CALCULATE
c
c This subroutine finds flowrates and enthalpy for standard
c Momotombo type of measurements.
c*****
c
    subroutine calculate (p0,ps,pu,pd,dd,d,h,
1  qs,qw,h_total,x_atm,x_sep,x_wh )
    implicit real*8 (a-h,o-z)
    real*8 t_sat_dp,h_vap_dp,h_liq_dp,v_vap_dp,b,alpha
    real*8 p0,ps,pu,pd,dd,d,h, qs,qw,h_total,x_atm,x_sep,x_wh
c
-----
c Coefficients of steam flow calculations, k as for saturated steam.
c The flow of steam calculated (equations 12 and 13 in report).
-----
c
    b = d / dd
    gamma = 1.13
    Y = 1. - ( 0.41+0.35*(b**4) ) * delp / (pu*gamma)
    call const ( b,alpha )
    tsat = t_sat_dp(pu+1.013)
    rho_s = 1./v_vap_dp(tsat)
    qs = 0.034783 * alpha * Y * dd*dd/100. * b*b * sqrt(rho_s*delp)

```

```

c
-----
c Coefficients of water flow calculations. The value 958 is the
c water density at 100 C in kg/m3 (equation 19 in report)
-----
c
    if ( h .gt. 0 ) then
        h = h/100.
        qw = 1.38 * 958. * ( (h+0.00085)**2.5 )
    else
        qw = 0.
    endif
c
-----
c Enthalpy calculations, h_total is the total enthalpy of the well,
c x_atm is steam fraction at atmospheric conditions, x_wh is the
c steam fraction at the wellhead and x_sep is the steam fraction
c in the separator (equations 20,21,22 in report)
-----
c
    tsat = t_sat_dp(ps+1.013)
    hl = h_liq_dp(tsat)
    x = ( hl - 417.5 ) / ( 2675.-417.5 )
    qw = qw/(1.-x)
    tsat = t_sat_dp(pu+1.013)
    hs = h_vap_dp(tsat)
    h_total = (hl*qw + hs*qs)/(qs+qw)
    if ( qw .gt. 0 ) then
        x_atm = ( h_total - 417.5 ) / ( 2675.-417.5 )
        tsat = t_sat_dp(p0+1.013)
        hl = h_liq_dp(tsat)
        hs = h_vap_dp(tsat)
        x_wh = ( h_total - hl ) / ( hs - hl )
        tsat = t_sat_dp(ps+1.013)
        hl = h_liq_dp(tsat)
        hs = h_vap_dp(tsat)
        x_sep = ( h_total - hl ) / ( hs - hl )
    else
        x_wh=1.
        x_sep=1.
        x_atm=1.
    endif
c
    return
    end
c
c*****
c          SUBROUTINE CONST
c
c This subroutine computes the value of alpha, according to
c equation 11 and 13 in report.
c*****
c
    subroutine const ( b,alpha )
    real*8 b,alpha,c
    c = 0.5959 + 0.0312*(b**2.1) - 0.184*(b**8)
    alpha = c / sqrt(1.-(b**4))
    return
    end

```

## Program MOM.F

```

c A program which calculates cumulative mass flow from the Momotombo
c geothermal field in Nicaragua. The input from input files are of the
c form
c   nud,ms,mw,h
c where nud = is number of day after jan 1st. 1987
c   ms = is mass flowrate of steam (kg/s)
c   mw = is mass flowrate of water (kg/s)
c   h = is total enthalpy of the fluid (kJ/kg)
c
c The program stores all these informations in matrixes, one for each well.
c After storing the informations, files of cumulative mass productions
c and time history of total fluid generation are made.
c
  program mom
  implicit none
  real ms,mw,h,j1,j2,j3,j4,j5,j6
  real ms_o,mw_o,h_o
  real as,aw,ah,bs,bw,bh
  integer nud,i,j,nud_o
  character*10 text
  character*60 name

c- input files
c
  write (6,('( Name of input file : ', $))
  read (5, '(a)') name
  open (unit=1, file=name, status='old')
  write (6,('( Name of output file : ', $))
  read (5, '(a)') name
  open (unit=2, file=name, status='unknown')

c
c- read the input
c
  read (1,*)
  read (1,*)
  read (1,*) text,nud_o,j1,ms_o,j2,mw_o,j3,j4,j5,h_o
c
  NUD_O = NUD_O - 60
  write (6, '(a12,i5,3f10.2)') text,nud_o,ms_o,mw_o,h_o
  do i=nud_o,1580
c
  read (1,*,end=200) text,nud,j1,ms,j2,mw,j3,j4,j5,h
c
  NUD = NUD - 60
  write (6, '(a12,i5,3f10.2)') text,nud,ms,mw,h
  if ( nud-nud_o .eq. 1 ) then
    write ( 2, '(i5,2f7.2,f7.1)') nud,ms,mw,h
  else
    as = ( ms-ms_o ) / ( nud-nud_o )
    bs = ms - as*nud
    aw = ( mw-mw_o ) / ( nud-nud_o )
    bw = mw - aw*nud
    ah = ( h-h_o ) / ( nud-nud_o )
    bh = h - ah*nud
    do j=nud_o+1,nud,1
      ms = as*j+bs
      mw = aw*j+bw
      h = ah*j+bh
      write ( 2, '(i5,2f7.2,f7.1)') j,ms,mw,h
    enddo
  endif
  nud_o = nud
  ms_o = ms
  mw_o = mw
  h_o = h
enddo
200 continue
stop
end

```

## Program CUM.F

```

c a program which calculates mass flow of steam and water from
c all momotombo geothermal wells. The input files contain columns
c with the day number after 01-jan-1987, mass flow of steam, mass flow
c of water and total enthalpy of the well. A sum of the mass flowrates
c from all wells is computed for each day and also the cumulative
c mass flow from the wells.
c
c-----
c                                     Grímur Björnsson, august, 1991
c-----
c
program cum
implicit none
integer i
real ms2,mw2,h2          ! steam flow, water flow and enth. of well 2
real ms12,mw12,h12
real ms17,mw17,h17
real ms20,mw20,h20
real ms22,mw22,h22
real ms23,mw23,h23
real ms26,mw26,h26
real ms27,mw27,h27
real ms31,mw31,h31
real ms35,mw35,h35
real m_s,m_w,m_t        ! total mass of steam, water and their sum
real c_s,c_w,c_t        ! cumulative masses
open ( unit= 1,file='inst.dat',status='unknown' )
open ( unit= 3,file=' cum.dat',status='unknown' )
open ( unit= 2,file='mt02.dat',status='old' )
open ( unit=12,file='mt12.dat',status='old' )
open ( unit=17,file='mt17.dat',status='old' )
open ( unit=20,file='mt20.dat',status='old' )
open ( unit=22,file='mt22.dat',status='old' )
open ( unit=23,file='mt23.dat',status='old' )
open ( unit=26,file='mt26.dat',status='old' )
open ( unit=27,file='mt27.dat',status='old' )
open ( unit=31,file='mt31.dat',status='old' )

```

```

open ( unit=35,file='mt35.dat',status='old' )
c
c- calculations perfermed for 1580 days in 1. day steps
c
c_s = 0
c_w = 0
c_t = 0
write (1,(' Day Steam Water Total'))
write (1,(' num (kg/s) (kg/s) (kg/s)'))
write (3,(' Day Steam Water Total'))
write (3,(' num (kg) (kg) (kg)'))
do i = 1,1580
read ( 2,('5x,2f7.2,f7.1')) ms2,mw2,h2
read (12,('5x,2f7.2,f7.1')) ms12,mw12,h12
read (17,('5x,2f7.2,f7.1')) ms17,mw17,h17
read (20,('5x,2f7.2,f7.1')) ms20,mw20,h20
read (22,('5x,2f7.2,f7.1')) ms22,mw22,h22
read (23,('5x,2f7.2,f7.1')) ms23,mw23,h23
read (26,('5x,2f7.2,f7.1')) ms26,mw26,h26
read (27,('5x,2f7.2,f7.1')) ms27,mw27,h27
read (31,('5x,2f7.2,f7.1')) ms31,mw31,h31
read (35,('5x,2f7.2,f7.1')) ms35,mw35,h35
m_s = ms2+ms12+ms17+ms20+ms22+ms23+26+ms27+ms31+ms35
m_w = mw2+mw12+mw17+mw20+mw22+mw23+26+mw27+mw31+mw35
m_t = m_s+m_w
c_s = m_s*86400 + c_s
c_w = m_w*86400 + c_w
c_t = c_t + m_w*86400 + m_s*86400
write (1,('i5,3f7.2')) i,m_s,m_w,m_t
write (3,('i5,3e12.5')) i,c_s,c_w,c_t
enddo
stop
end

```